TAMPERE UNIVERSITY
OF APPLIED SCIENCES

Further development of a solar thermal chamber dryer for fish

Based on a previous device

Lisa Josefina Eva Büscher

Bachelor's thesis
08.05.2018
Energy- and Environmental Engineering
Verfahrens-, Energie- und Umwelttechnik

ABSTRACT

Tampereen ammattikorkeakoulu
Tampere University of Applied Sciences
Energy- and Environmental Engineering
University of Applied Sciences and Arts Hannover
Verfahrens-, Energie- und Umwelttechnik

Author: Lisa Josefina Eva Büscher
Further development of a solar thermal chamber dryer for fish
Based on a previous device

Bachelor's thesis 41 pages, appendices 22 pages
08.05.2018

In this final thesis, a drying chamber has been developed, on the basis of a previous prototype.
A new design has been drawn in Inventor 2018 and has been tested then in Autodesk CFD 2018, to figure out air flow problems beforehand. Additional, first calculation has been done, to examine the running conditions.
To improve the air flow, the drawers have been staggered in reverse order. The CFD Analysis has shown, that there were still air flow problems in the lower levels of the chamber. The air did not flow equally up but had to distribute during the up flow from the middle to the edges. This led to the creation of a vortex in the lower levels and, therefore, to a flow of the air in the wrong direction, from the backside of the chamber to its front. To prevent an unequal drying by this, changes in the design has been done. After adding a deflection plate in the ground of the device in front of the inlet and of plates to the drawers, the problems have been solved. The calculations have shown, that the drying will need 6 h, while the air flow rate at the inlet is about $0{,}1\,\frac{m^3}{s}$.
The next step will be to build a new prototype and to do further testing. Especially the air flow rate and the drying time has to be tested, because the calculations are based on assumptions.

Diese Bachelorarbeit beschäftigt sich mit der Entwicklung einer solarbetriebenen Kammertrockenanlage für Fisch. Das neue Design wurde auf Basis eines bereits getesteten Prototyps entwickelt. Zur Verbesserung der Luftströmung wurden die Trocknungsebenen versetzt zueinander angeordnet, wodurch frische Luft jede Ebene zur selben Zeit durchströmt. Eine CFD Analyse ergab jedoch Probleme bei der Luftströmung in den unteren Ebenen. Die Luft strömte nicht einheitlich nach oben, sondern sich von der Mitte zu den Seiten verteilend. Sie war nicht einheitlich über den Querschnitt verteilt. Dadurch ergab sich das Problem, dass die Luft in den unteren Ebenen an den Seiten einströmte, wodurch sich innerhalb einer Ebene Strudel ausbildeten. Die Luft strömte also nicht wie vorgesehen von vorne nach hinten, sondern in der Mitte der Ebene von hinten nach vorne. Um eine ungleichmäßige Trocknung des Fisches hierdurch zu verhindern, wurde das Design erneut optimiert. Im unteren Teil der Anlage, im Bereich des Lufteinlasses, wurde ein Aufprallblech installiert, welches für eine frühere Verteilung der Luft sorgt. Darüber hinaus wird nun durch zusätzliche Bleche, die als Strombrecher fungieren, in den Schubladen das Ausbilden von Wirbeln verhindert. Durch diese Maßnahmen konnten die Probleme gelöst werden und eine gleichmäßigere Trocknung des Fisches ist möglich.

Zusätzlich wurden erste grobe Berechnungen der Trocknungszeit und des benötigten Volumenstroms durchgeführt. Für die Dauer des Prozesses ergab sich eine ungefähre Zeit von 6 h und für den Volumenstrom ein ungefährer Wert von 0,1 $\frac{m^3}{s}$.

CONTENTS

ABBREVIATIONS AND TERMS

A	Area for drying [m²]
A, B, K	Parameters of equation (2) [-]
c_p	Specific heat at constant presure [kJ/(kg*K)]
D_e	Equivalent diameter of channel [m]
EMC	Equilibrium moisture content [kg_W/kg_A]
ERH	Equilibrium relative humidity [%]
h_y	Heat-transfer coefficient between gas and surface of slap [W/m²]
L_P	Perimeter in contact with fluid [m]
$\dot{m}$	Mass flow [kg/s]
m	Mass [kg]; m_s, Mass of solid
p	Partial water vapour pressure [Pa]
p_0	Partial water pressure at saturation [Pa]
Pr	Prandtl number [-]
$\dot{Q}$	Heat flow [W]
r	Latent heat of vaporization [J/kg]
r_H	Hydraulic radius [m]
R_c	Rate of drying in constant rate period [kg/(m²*h)]
Re	Reynolds number [-]
S	Cross sectional area [m²]
T	Temperature [K]; T_i, temperature at interface
w	velocity of the stream [m²/s]
X	Moisture content [kg_W/kg_A]; X_c, moisture content at critical point

Greek letters

α_w	Water activity [-]
η	Viscosity [kg/(m*s)]
λ	Thermal conductivity [W/m]
ρ_F	Density of the fluid [kg/m³]
φ	Relative humidity [%]

Subscripts

A	Air
F	Fish
W	Water
α	Inlet/ in the beginning
ω	Outlet/ in the end

1 Introduction

This work is about the planning of a solar thermal fish dryer and has been done in cooperation with the company Solar Fire Concentration Oy.

This company has planned and implemented other solar thermal driven devices in Africa already. Their devices are based on the reflection and the focusing of the sun radiation into a certain device, like an oven. Therefore, the mirrors are curved and arranged in a special way, which cannot be described further, due to confidentially issues.

As another method of utilization of the sun energy, a dryer for fish will be planned.

Drying is a common method for food preservation. By reducing the moisture content of a product, goods like vegetables, crops, meat and fish spoil slower. The heat, which is needed for this process, can be supplied either for example by a fire or traditionally by the sun. This solar drying is still common in sunny countries, like in Africa. Often the farmers or fishers are using no special device for it, but the drying takes place at the open air on the ground. The problem by this kind of drying is the dependence on the natural influences. The drying needs up to several days and at the same time the food is exposed to all kind of animals and insects. The consequence are losses.

To prevent this and to improve the efficiency of the drying, several different types of solar drying devices are applicable. Depending on the product, one type has to be chosen.

The aim of this final thesis is the development of a design for a solar thermal fish dryer. This dryer consists out of two units: the dryer and the heat exchanger. In this work, the dryer is constructed in the program Inventor 2018. This happens on the base of the already build and tested prototype. After developing a design and a rough calculation of the running parameters, the air flow will be simulated in Autodesk CFD 2018. The results will be analysed, to obtain possible problems of the design. If something occurs, the design will be changed until the results of the analysis are satisfying. Assembly drawing will be made out of the final design.

2 Theory

2.1. Drying

The drying process is the removal of a liquid component from a humid good by evaporation or volatilization. The good can be solid, pulp or liquid and the process can be done by mechanical or thermal processing. [1]

Through the thermal drying, transferring of energy and material takes place. The heat flow $\dot{Q}$ gets transferred from the drying agent to the material to be dried. The moisture content of the good gets reduced. This happens by the heat flow, which warms up the water of the good until it changes from liquid to gaseous. [1]

By the evaporation, the drying agent consists at least out of two gases. One of these is the gaseous humidity of the good, commonly steam and the other is generally air. Thereby, the air is the supplier of the energy. [1]

By the volatilization consists the drying agent out of the substance, which has to be removed. If this is water, the agent is steam. [1]

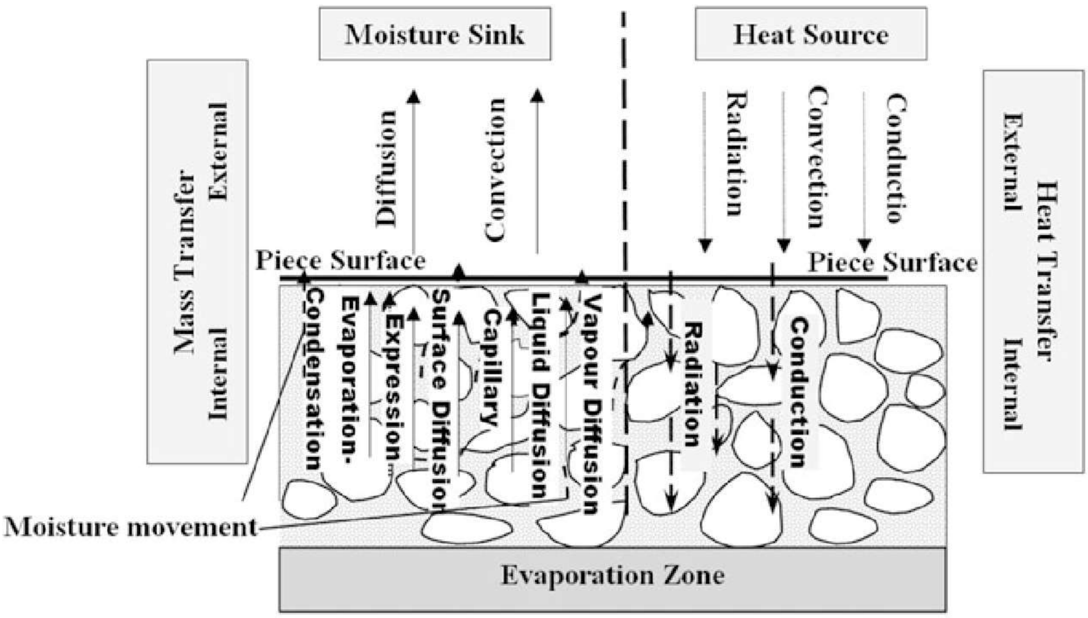

Figure 1: Rate factors in drying [2]

The drying process can be divided generally into two mechanisms: the heat transfer (right side of Figure 1) and the mass transfer (left side of Figure 1). The driving force of the drying process is the pressure gradient between the product and the air. The vapour pressure of the product, increased due to the evaporated moisture, is higher than the one of the surrounding. This leads to the external mass transfer, so to the transfer of the moisture from the product surface to the surrounding by diffusion or convection, like shown in Figure 1. More water gets supplied by the movement of moisture from the inside the product to his surface. This process is called internal mass transfer. This is caused by the capillary flow, flow by gravity and other kinds, which are listed in Figure 1. The heat transfer is generally caused either by radiation, convection or conduction, while convection is most common. [2]

2.1.1 Convection drying

By the convection drying, the energy transfer takes place between the hot air and the product surface. The heating of the air can be operated by any heat source. The water from the surface volatilizes, caused by the conduction of this energy. The removing of this steam happens by air movements. The removal of the surface water causes a migration of internal water to the surface. [2]

2.1.2 Drying curves

In Figure 2 different drying curves are shown. The variation of the moisture content over time can be determined during the drying process. Out of this, the drying rate can be calculated. The drying rate is defined as “the mass of water removed per unit time per unit mass of dry material or the mass of water removed per unit time per unit area” [2, p. 23]. The drying rate curves are for every product unique, since they depend on the type of material and its structure. Nevertheless, they are very important for determining the behaviour of the product during the drying process. [2]

The idealised drying curve can be divided in three Phases. Before the first one, from point A to B, the heating of the product up to the drying

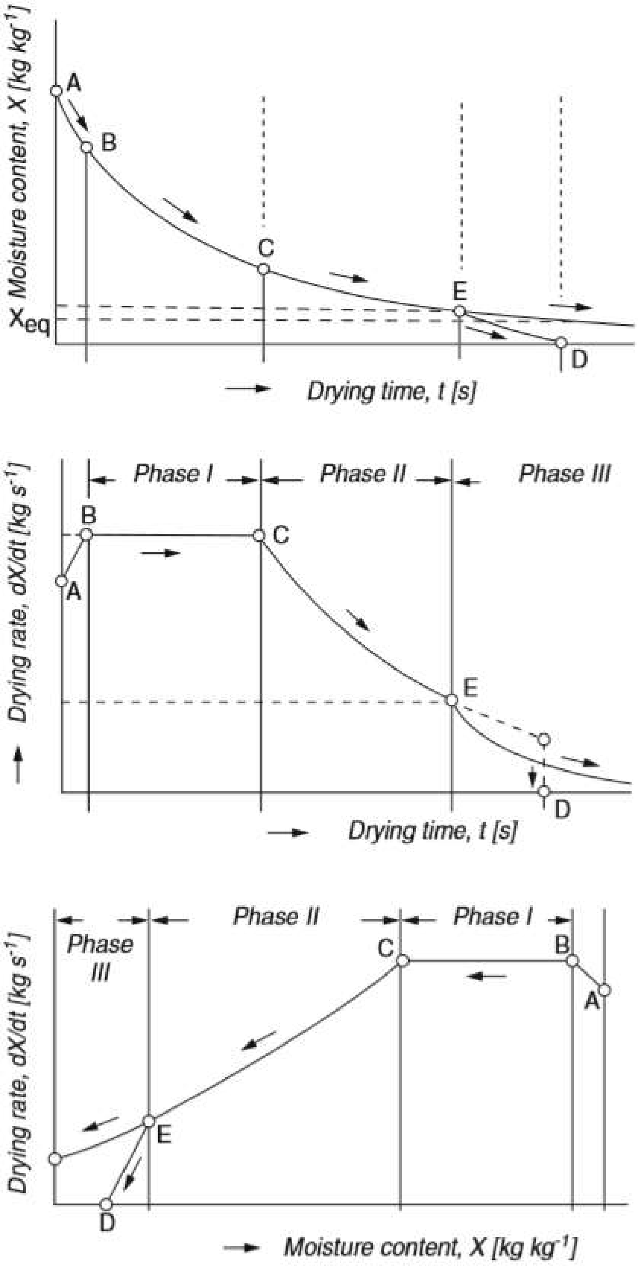

Figure 2: The drying curves [2]

temperature takes place. The first phase (B to C) is the initial constant rate period. During this, the evaporation takes place continuously, because the surface of the product is saturated with vapour. The drying rate of the phase is called the constant-rate period drying rate R_c and ends with the moisture content X_c at the critical point C. Phase II takes place from C – E and is the first falling-rate period. The surface is now unsaturated and internal liquid movement is going on. The drying rate reduces at a steady state. For Non-Hygroscopic materials, this takes place until the moisture content reaches zero. For Hygroscopic materials Phase III, the second falling-rate period, starts from point E. Now the moisture content decreases slower until it reaches the equilibrium moisture content EMC (point D) and drying stops. In this point, the product absorbs as much moisture from the air, as the air takes away from the product. The vapour water pressure in the product is equal to the one in the surrounding air. [2], [3]

2.1.3 The water activity

The water activity α_w is defined as the ratio of the partial pressure of water vapour over the wet product at a specific temperature and the partial pressure of pure water at saturation at the same temperature (cf. Equation (1)). It is equal to the relative humidity φ of the product. Consequently, the relative humidity of the product is at the equilibrium moisture content EMC identical to the relative humidity of the surrounding air and known as equilibrium relative humidity ERH. [2]

$$\alpha_w = \frac{p}{p_0} = \varphi \qquad (1)$$

The water activity is an important parameter in food storage, because it indicates the availability of free water in the product. This water causes mainly the deterioration of food, by taking part in chemical reactions, growth of microorganisms and spore germinations. In Figure 3 is shown, which activities (chemical, microbial or enzymatic) needs which water activities for taking place.

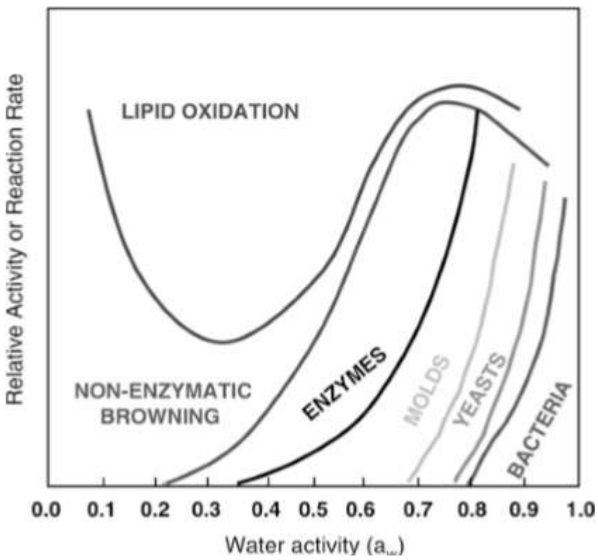

Figure 3: Water activity - stability diagram [2]

So, chemical reactions are the only influence on the quality of the product under the water activity of 0,7. Over 0,7, moulds, yeasts, bacteria and other microorganisms affect the quality mainly. [2]

2.1.4 Sorption Isotherms

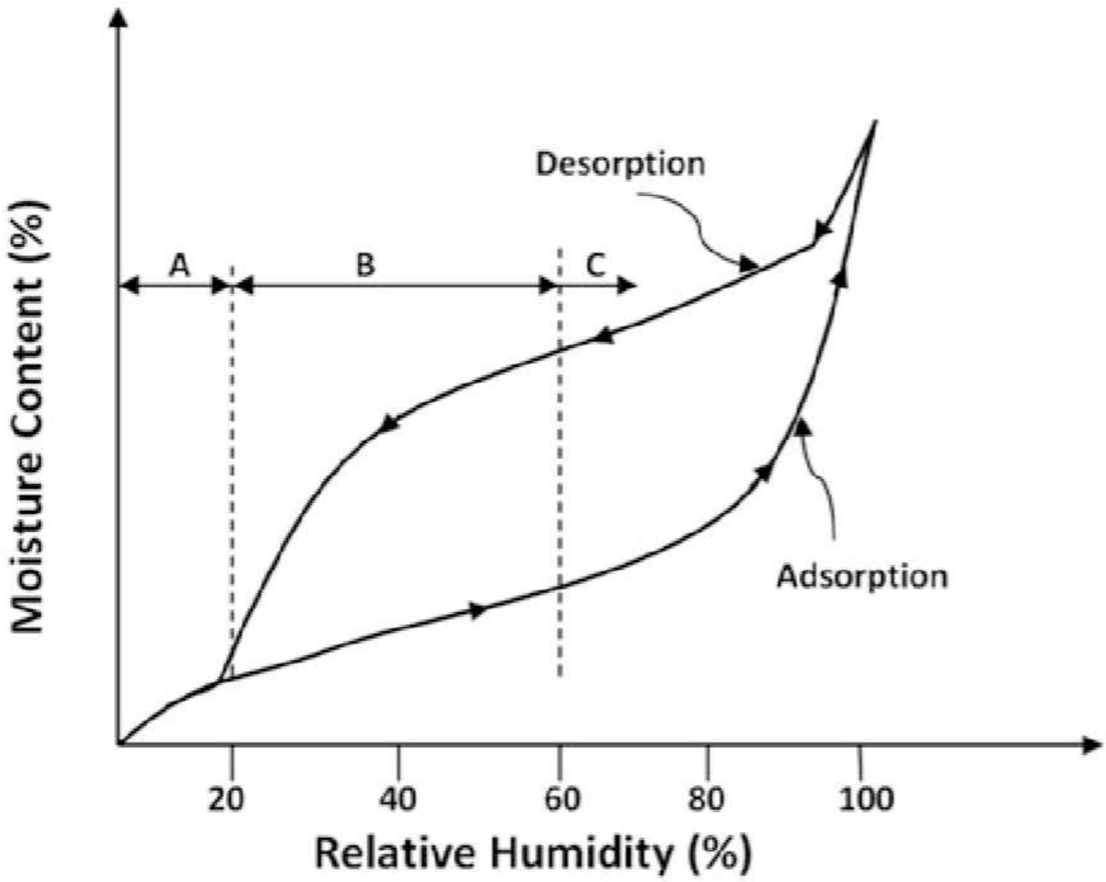

Figure 4: Typical sorption isotherm showing hysteresis loop [2]

Sorption isotherms describe the relationship of the moisture content of a product to the corresponding water activity. Figure 4 shows an example of a sorption isotherm. The desorption happens with a slight hysteresis in comparison to the adsorption. The process of ad- or desorption is based on the gradient of partial pressure of water vapour between the air and the product to be dried. If the partial pressure of the product is higher, the moisture transfers from the solid to the air, the adsorption takes place, and opposite for desorption. [2]

Depending on binding mechanisms, the graph can be divided into three parts. In region C, the water is bound. This water is linked only loose and is available for reactions. Zone B is the transition zone. The water is still bound loosely but is now located in smaller capillaries. Nevertheless, it is still free water and so accessible for reactions. The water in section A is unavailable for reaction, since it is bound to the solid through adsorption mechanisms. [2]

Many different mathematical equations are existing to describe the sorption process. Most common for food processing are the BET and GAB equation. The BET equation is a modification of the model of Langmuir, a molecular monolayer equation. This model is applicable for $0{,}05 < \alpha_w < 0{,}45$. The GAB equation is more widely accepted and represented, because it is suitable for water activities from 0,1 to 0,9. The formula is shown below:

$$X = \frac{A * B * K * \alpha_w}{(1 - K * \alpha_w) * (1 + (B - 1) * K * \alpha_w)} \quad (2)\ [4]$$

X describes the moisture content of the product in $\frac{kg_W}{kg_A}$ and A, B and K are parameters, which has to be determined experimentally. They are depending on the temperature during the adsorption. [3]

2.1.5 Thin layer and deep bed drying

Besides the properties of the product itself, the thickness of the drying bed has a huge influence on the drying rate. Depending on the product, it can be either dried in thin layers or in a deep bed. [3]

Most products, such as fruits and vegetables, are dried in thin layers. For this the simplification can be made, that the ratio of air volume to the good volume is infinitely large. So, the drying rate depends only on the properties of the material, its size, the drying air temperature and the moisture content. [3]

For the drying of corn, beans, etc. deep bed dryers are common. These smaller products can be dried in a continuous bed, by passing air through it. In this type of drying the process takes place in zones. The lower zone dries rapidly, and the air moves up, while the moisture content increases and the temperature falls. This leads to a gradient in temperature and moisture content between the lower and the upper zone. Besides the air flow rate and drying air temperature, is the bed's depth a critical factor of the drying. [3]

2.2. Solar Drying Systems

Solar Dryers can be classified by various modes, e.g. by the type, the operation temperature, the material to be dried or the operating mode (batch or continues). In Figure 5 one possibility based on design and mode is shown.

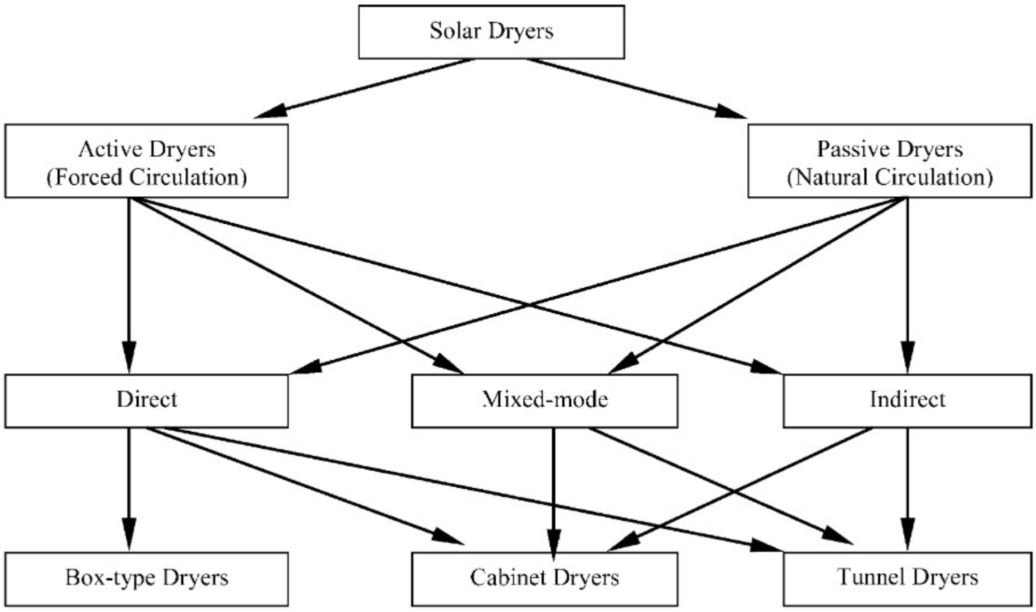

Figure 5: Classification of solar dryers and drying modes [5]

The solar dryers can be separated mainly into the passive and active dryers. The convection by the passive ones is natural. This means, that the heated air circulates freely due to buoyancy force and/ or as a result of the wind pressure. If the convection is forced, the dryer is called active. To create the forced air flow, a fan can be used. The power for this can be supplied by photovoltaic. The advantages are an improved airflow and higher drying rates. But at the same time, these kinds of dryers are more complex and thereby more expensive. [2]

In Figure 6 can be seen, how the moisture content changes during the drying process, depending on the air flow. Open-air sun drying has the lowest decline of moisture content during the time. The active dryer is the fastest. For example, after 20 hours of drying the moisture content of the chillies in a forced convection dryer is about 0,1 %. The moisture content of the ones of the open-air sun drying is with approximately 1 % higher. Therefore, a wanted moisture content can be reached with an active dryer faster than with a passive one or with open-air sun drying. [2]

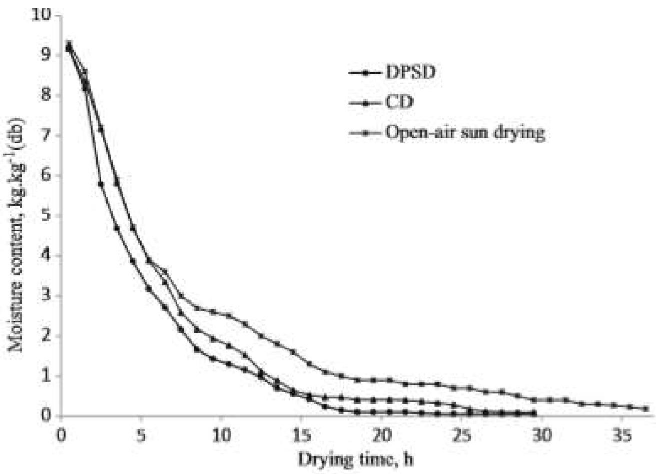

Figure 6: Changes of moisture content of red chili with drying time. DPSD double-pass solar dryer (forced convection dryer); CD typical natural convection cabinet dryer [16]

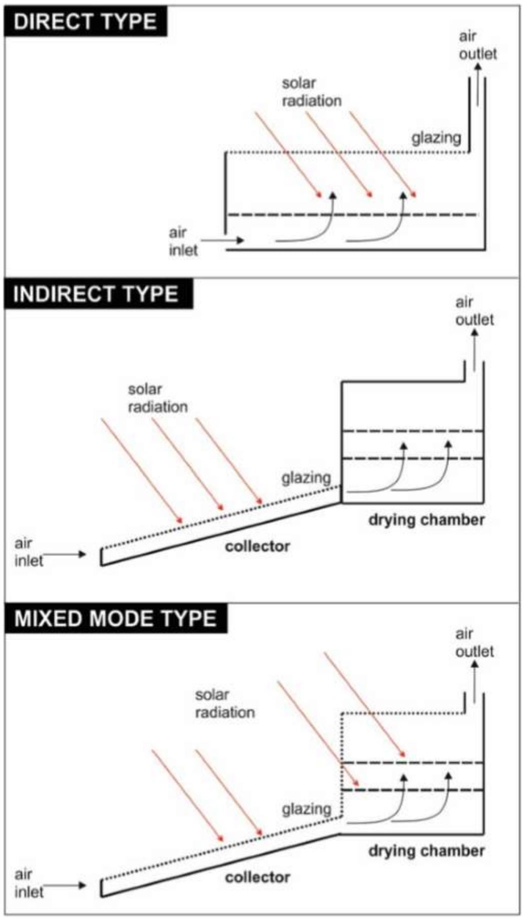

Figure 7: Working principle of direct, indirect, and mixed-mode solar dryers [2]

Direct solar drying means, that the radiation heats directly the material (cf. Figure 7). This can happen either outdoor by direct incidence solar radiation, or through a transparent cover, which partly protects the product from natural influences, like weather or insects. [3] The direct exposure to the sun light can be important for the product. These causes the required colour and flavour of certain products, like some crops and coffee. In general, is this type of drying simpler and less expensive. The problem is, that a locally or relatively overheating might be possible. [2]

The working principle of the indirect solar drying can be seen in Figure 7. The dryer has some thermal energy collecting devices and is not transparent [3]. The product heats up by the circulating air. These kind of drying gets often applicated for sensitive products. The structure of the dryer is more complex and therefore, the investment costs are higher. The running is more expensive, too. [2] However, the operation of indirect dryers is based often on experience [3].

The mixed mode type of solar dryer function as a combination of the direct and indirect one, as shown in Figure 7. Problematic is, to achieve a constant temperature for drying. The air, which leaves the collector heated up, has no constant temperature but it varies highly. [2]

2.2.1 Open-air Sun Drying

The open-air sun drying is the oldest type of drying. The product gets spread in a thin layer on a large outdoor surface. The solar radiation heats directly the material, while the air movement is created by density differences. Therefore, the open-air sun drying is direct and passive. The drying rate is very low, for example for crops, the drying can last 10 – 30 days. The drying depends highly on natural influences, like the weather conditions, solar radiation intensity and on the environmental wind velocity. Even if the product is covered by for example a removable plastic cover, it is a subject to weather and natural attacks, like insects or birds. All this leads to losses in quantity and quality. Another problem is, that the quality cannot be controlled in a proper way. The process is based on the experience of the unskilled personnel. Nevertheless, the open-air sun drying is an economical drying procedure, which needs only small initial capital. For this reason, many small farmers in developing countries are still using this technique for the drying of their product. [3]

2.2.2 Chamber Dryer

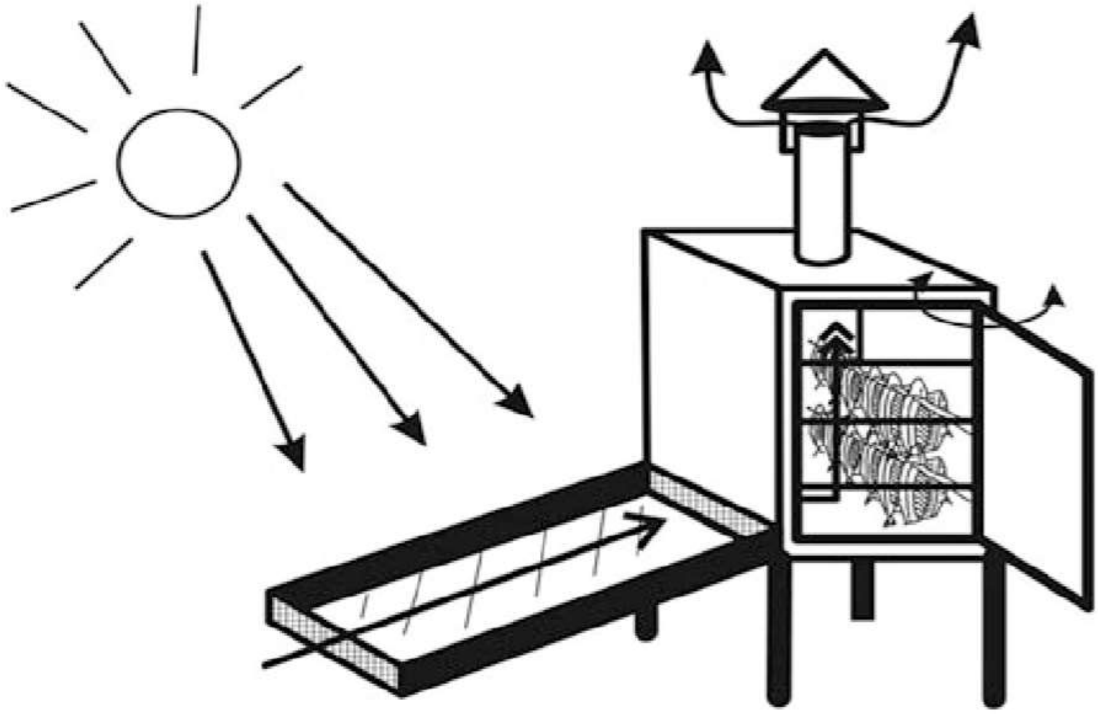

Figure 8: Natural convection chamber dryer [2]

Chamber dryers have a higher capacity, compared to one-layer dryers. Several drawers are accommodated on top of each other in a chamber, so that a multi-layer bed gets created. As shown in Figure 8, the air is heated up by the sun, before it enters the chamber. Here, an indirect dryer is shown, even though mixed-mode dryers are applicable. Therefore, a transparent cover can be used for the chamber. This might be necessary, to achieve special properties for special products, like for coffee. A natural circulation can be generated by the chimney, using the ”chimney effect”. The chamber dryer can be also converted to an active dryer by adding a ventilator. [3]

3 Boundary conditions

3.1. Fish

The fish, which has to be dried is the "Rastrineobola argentea", locally known as Dagaa. This fish is a subspecies of the sardines and can be found among other locations in Lake Victoria.

Sardines are small fish of the herring family [6]. Dagaa has an initial moisture content of $72{,}83\ \% - 76{,}90\ \%$ [7], so in average about $75\ \%$. After the drying, the final moisture content has to be $15\ \%$ [2]. In average the Dagaa has a length of $4{,}6 \pm 0{,}34\ cm$ [7].

In general, sardines are rich on different nutrients, like Omega-3 fatty acids, B vitamins, vitamin D, calcium, phosphorus and protein. [6] The amount of the nutrients per 100 g and the percentage of the minimum recommended daily intake for sardines of the Atlantic of each nutrient is listed in the Appendix 1. As theses sardines, are the Dagaa rich in proteins, minerals and lipids, as well [7].

Vitamin D is one of the nutrients, which are available in a high amount in sardines (100 g provides about 68 % of the recommended daily intake). This vitamin is especially important for the bones. A deficiency can cause for example osteoporosis. [6] The amount of Vitamin D_3 can be influenced highly by solar drying. By the influence of direct sun radiation this Vitamin gets reduced for the most part. [8]

The drying rate curves for different drying conditions of sardine muscles are shown in Figure 9. The temperature of the air has a major influence on the drying process. The influence of the relative humidity (RH) and the velocity of the air (v_a) is less significant but still an important factor for the drying efficiency. The curves also show, that the drying of sardine muscles has no initial constant rate period. The drying starts with the first falling period. This indicates, that the moisture movement inside of the fish is governed by diffusion. [9]

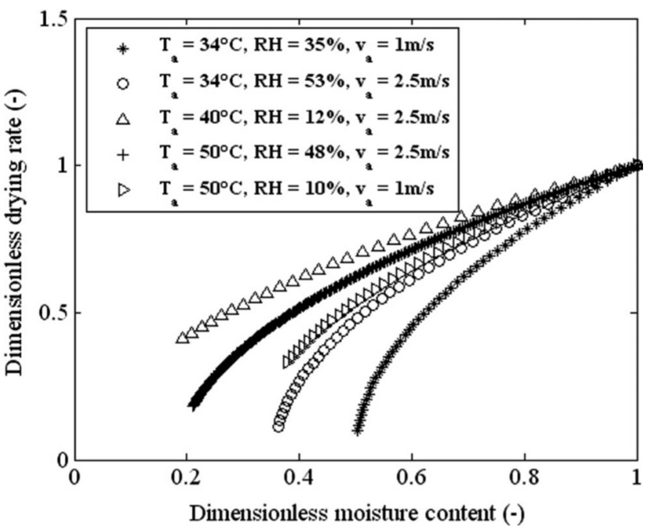

Figure 9: Variation of dimensionless drying rate of sardine muscles versus reduced moisture at various air conditions [9]

3.2. The location

The first prototype was installed at Bao Beach at Lake Victoria in Kenya. The following figures show the average temperature (Figure 10), the average monthly hours of sunshine (Figure 11) and the average air humidity (Figure 12) over the year, recorded of the nearest weather station in Nakaru, Kenya. Especially the hours of sunshine and the air humidity are important factors for the drying process. How long the device can run per day is governed by the hours of sun per day. The humidity of the air is important for the efficiency of the drying process. The lower the relative humidity, the more moisture can be removed during the drying process. If the relative humidity is about 100 %, a drying process cannot take place. The relative humidity is in average 60 % in Kenya. This will be even lowered by an increasing of the temperature, in the heat exchanger.

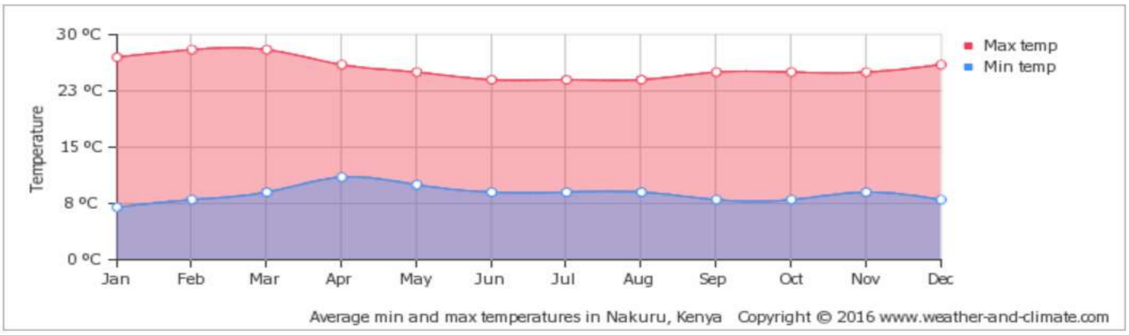

Figure 10: Average minimum and maximum temperature over the year (Nakaru, Kenya) [10]

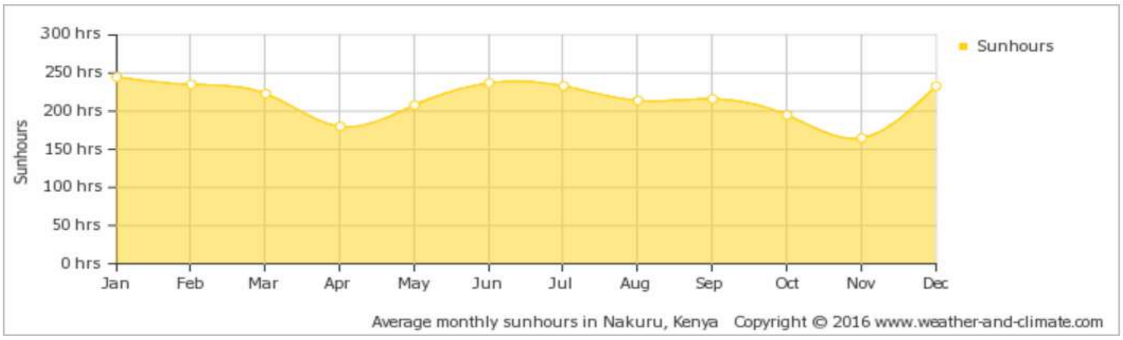

Figure 11: Average monthly hours of sunshine over the year (Nakaru, Kenya) [10]

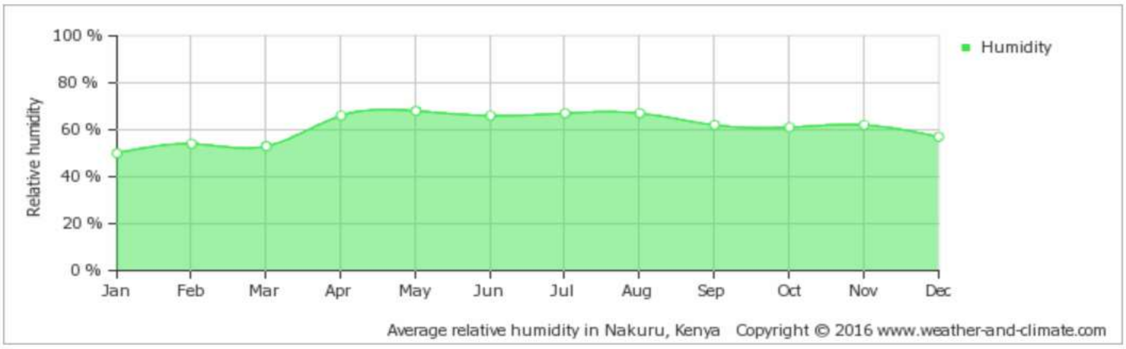

Figure 12: Average humidity over the year (Nakaru, Kenya) [10]

4 Existing Prototype

4.1. Design

The first Prototype of the solar thermal dryer is a chamber dryer. The radiation of the sun becomes reflected by mirrors into the bottom of the chamber. The chamber is designed as a box, made out of metal. In the bottom of the device are several rocks. They are, on the one hand, a weight, to put the centre of gravity of the chamber more down. On the other hand, they operate as a heat exchanger. The radiation, which gets focused by the mirrors, heats up the rocks and they heat up the surrounding air again. Figure 13 shows a picture of the drying chamber of the prototype.

In the upper part of the chamber, above the stones, are several drawers located. They are arranged directly above each other. The fish lays on these trays during the drying. The chamber is equipped with a chimney on the top. This has an integrated fan, to create a forced convection.

Figure 13: Loading of the first Prototype [11]

4.2. Problems

The prototype has several problems. The heat exchanger has to be improved to increase the efficiency. The focus lays on finding a more efficient material or fluid for that. The other weakness of the current design in the air flow inside of the chamber. The fish is drying such irregularly, that the drawers has to be changed several times during the drying process.

The irregular drying occurs due to bad air flow. Because of the arrangement of the drawers inside of the chamber, the fresh air cannot be distributed equally. The air has to pass first the lower drawers before it reaches the upper ones. During this process, the air gets saturated with moisture, before it arrives at the upper drawers. The saturated air is not able to absorb any more humidity from the fish. On account of this, the shrinking of the amount of water of the fish in the upper levels is much slower than in the lower ones.

5 Assessment criteria

The parameters, which influence the drying process mainly, are the drying air characteristics, product variables and dimensional variables of the dryer. These are listed in detail below in Table 1. For the evaluation of a dryer and the drying process these parameters have to be taken into consideration. [5]

Table 1: Influencing parameters on the dryer performance

Drying air	Product variables	Dimensional variables
• Temperature • Humidity • Air flow	• Throughput • Initial and final moisture content • Product size distribution	• Width • Length • Height/ diameter • Number of passes • Dryer configuration

The evaluation can be divided into different categories [5]:

- Physical features of the dryer
- Thermal performance
- Quality of the dried product
- Cost of dried product

For this work especially important are the physical features of the dryer and in part the thermal performance. Other parameters, like the quality of the dried product, can be only obtained by running the dryer.

5.1. Design criteria

For the design the physical features of the dryer are important. This includes the type, size and shape of the dryer, the drying capacity/ loading density, the tray area and number of trays and the loading/ unloading convenience. [5]

The physical size of the dryer is directly related to the capacity, so the quantity dried in a single batch, measured in kg of fresh product per batch. Thereby, the throughput describes the amount of wet product, which can be dried to a required moisture content. This gets expressed usually in kg fresh product per day. The tray area and number of trays influences the capacity of the dryer, as well. Most efficient is to spread the product in one layer on the tray. So, the available drying area depends on the size of each tray and on their number. The loading density is as important for the capacity as total tray area and drying time. On the one hand, an over-loading, for example by placing more than one layer above

each other, limits the surface and results in poor drying and a negative influence on the quality of the dried product. On the other hand, a part loading also reduces the drying efficiency, because of a resulting non-optimal utilisation of aperture are. [5]
Besides the capacity as design criteria, the handling is very important. The loading and unloading of the product has to be as simple as possible. The extraction and insertion of the trays should be possible without any big problems or actions, like unscrewing of parts. The installation and maintaining has to be easy, as well, so that no professionals are needed for that. In general, the device should be as simple as possible, so the investment costs are as low as possible. The dryer has to be affordable for the fishers.

5.2. Air Flow criteria

The thermal performance includes the parameters drying time/ drying rate, temperature and relative humidity of the drying air, airflow rate and dryer efficiency. Air flow is indirect a part of it, because it influences significant the drying efficiency. The more equal the air flow, the higher the drying efficiency. [5]
The drying air is entering the drying chamber already with the required properties, like velocity, temperature and humidity. It does not get regulated by the drying chamber, but by the upstream connected heat exchanger.
The dryer efficiency and also the drying time depends on the air flow. Important is, that the "fresh" air enters all drawers, to prevent irregular drying. If the air has to pass the lower tray to reach the upper ones, a deep bed gets created. Consequently, the food on the upper trays will dry slower. This has to be prevented. The good in the whole chamber should have the same drying time and therefore, "fresh" air in nearly the same amount should enters each tray. Also, the velocity of the air has to be nearly the same in each level.

6 New Design

The basically design of the prototype should remain. The chamber dryer has the advantage of a high capacity, due to the several trays located on top of each other.

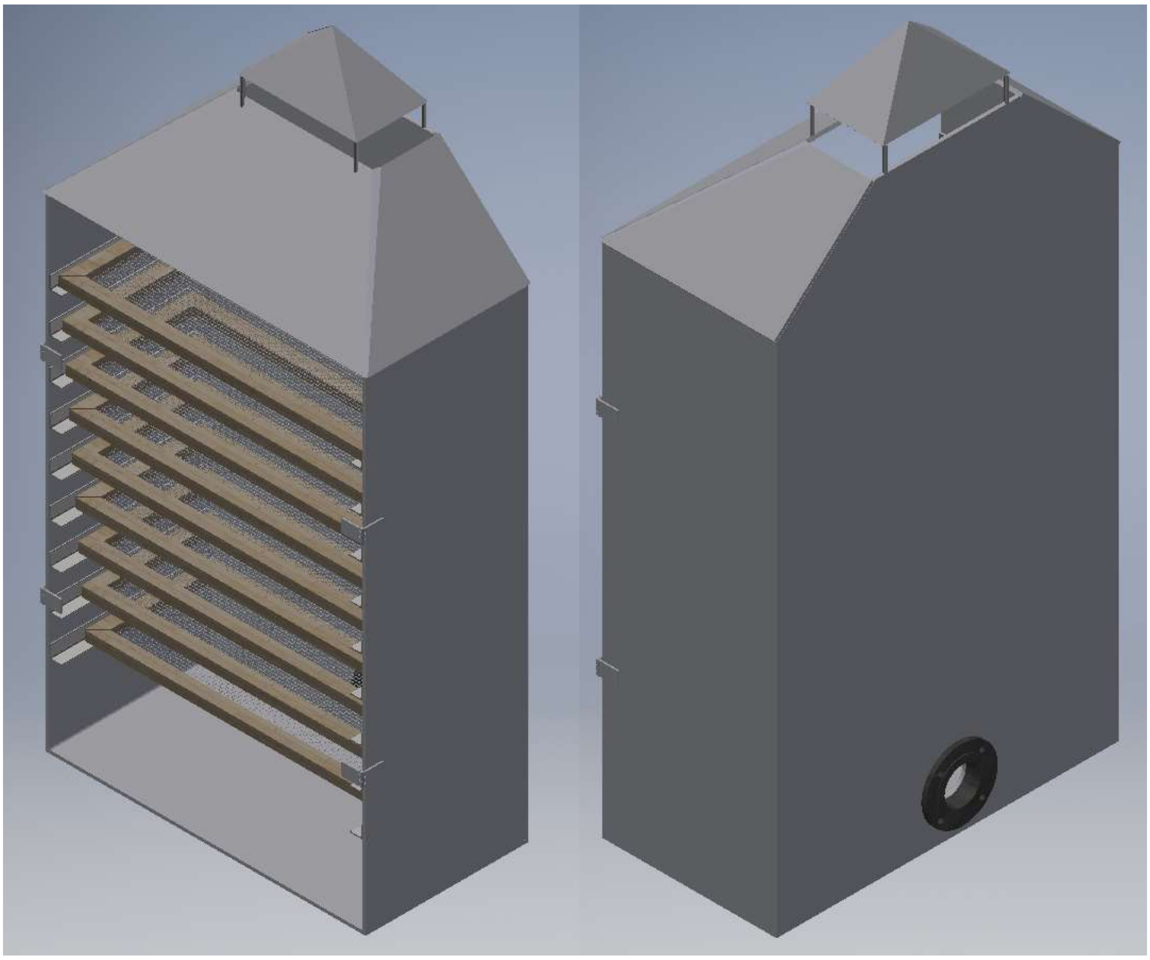

Figure 14: Isometric point of views of the new design of the drying chamber

Figure 14 shows the new design. The length is $1\ m$, the depth $0{,}5\ m$ and the total high about $2\ m$, while the highest tray is at $1{,}3\ m$. The non-quadratic size was chosen to ensure a more equal drying in the depth of each drawer. If the depth is too big, the air is already saturated, when it reaches the end of the drawer and no drying can take place there. At the same time, the capacity should be as big as possible, therefore the length is bigger than the depth. Still important is the handling of the trays. To ensure, that one person can carry one tray alone, the length should not be too big. Similar applies for the high of the chamber. The inlet of the air is at the back of the chamber. The heated air enters through a pipe, coming from the heat exchanger. To connect both devices, a V-Flange is attached at the air inlet.

The energy supply takes place only indirect. A direct exposure of the fish to the sun, would cause degradation in quality. Like mentioned in chapter 3.1, the direct radiation would cause a reduction of important nutrients. Consequently, the drying will take place only indirect.

The fresh air flows from the back of the chamber to the front, where it rises upwards. To guarantee, that this air enters each level, the trays are staggered in reverse order. The outlet of the air is at the top of the chamber. The cross-section reduces, to have a smooth outflow of the air, with as less turbulence as possible. A little roof, which is based on four round bars, secure protection to environmental influences, like rain.

The doors are affixed with weldable hinges. The chamber can be closed by a lever. It is pivoted-mounted at the one door and hooks on the other door.

Because of the high humidity, which the air will have after the drying, the chamber should consist mainly out of stainless steel, to prevent corrosion. Suitable would be the X8CrNiS18-9 with the material number 1.4305. This kind of stainless steel is applicable especially for parts in the food industry [12]. The drawer itself will consist out of the same material as by the first prototype. There, the frame was out of wood and the mesh out of plastic, to prevent sticking of the fish at the mesh after the drying. This has happened, because a metal mesh heats up during the drying, as well. By using plastic as a material, this can be prevented. Here is only important to choose a material, which is food safe.

7 Calculations

These calculations have the objective to give an estimation about operating data, like drying time and air flow. Due to the early stage of developing and missing data, the results serve as an estimation. The aim is to receive a basic knowledge about the operation.

7.1. Sorption Isotherm

The sorption isotherm of the fish can be calculated by the GAB equation (2). The parameters A, B and K have to be determined for that. For the "Rastrineobola argentea" no study about the sorption isotherm has been found. Therefore, the parameters for the GAB equation of small silverside fish were taken. The size ($8{,}05 \pm 0{,}3\ cm$ x $1{,}2 \pm 0{,}3\ cm$) and moisture content (73 ± 3 %) is roughly the same as for the sardines. This leads to the conclusion, that the sorption isotherms will not differ much. Because of the only rough calculations, this lead not to major variations in the results. The parameters for three different temperatures are listed in Table 2. The resulting sorption isotherms are shown in Figure 15.

Table 2: Parameters for the GAB equation for different temperatures [4]

	T=50	T=60	T=70
A	0,255	0,0984	0,0885
B	0,5874	0,8059	0,7165
K	0,8891	0,9406	0,9721

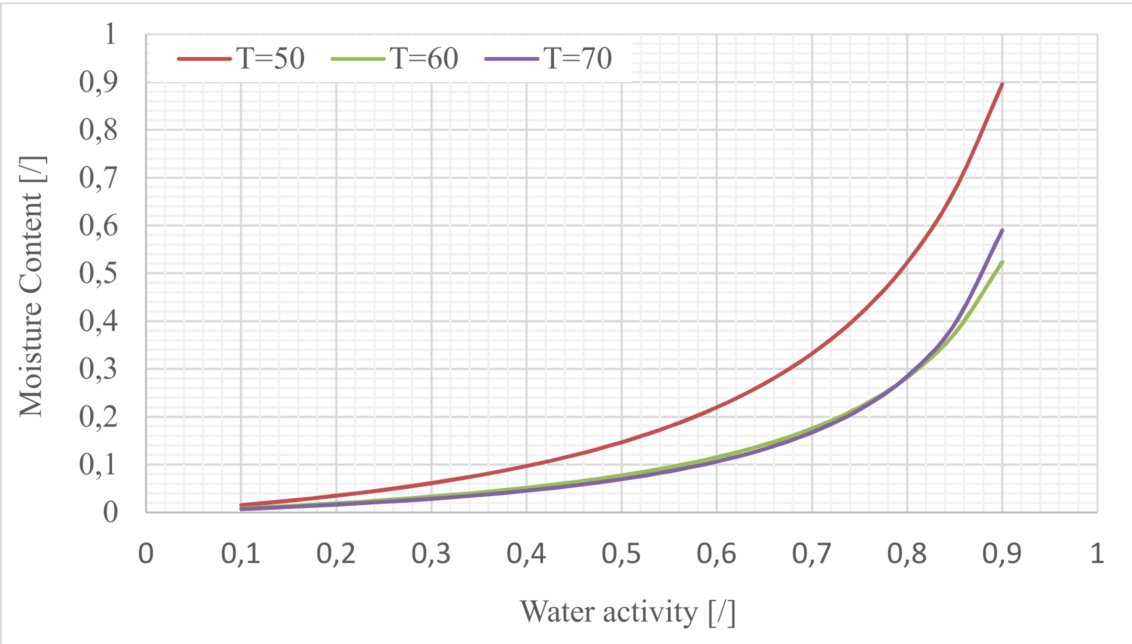

Figure 15: Sorption isotherm for fish by different temperatures

7.2. The process in the h, x - Diagram

By charting a process in the h, x – Diagram, the properties of the air can be examined at different points of the process. The behaviour of the drying air during the process is shown in Figure 16. The process starts at point 1, the inlet of the heat exchanger. The air is the ambient air, which has an average temperature of $25\ °C$ (cf. Figure 10) and an average relative humidity of $60\ \%$ (cf. Figure 12). In the heat exchanger, the air gets heated up to $50\ °C$ (point 2). This process takes place without any change of the absolute moisture content, which remains at $11{,}9\,\frac{g_W}{kg_A}$. From Point 2 to 3, the drying takes place. The relative humidity of the air rises from $15{,}4\ \%$ up to $87\ \%$, while the temperature drops to $28\ °C$. During this process the assumption is made, that the specific enthalpy does not change. The final moisture content or equilibrium relative humidity of the air can be examined out of the sorption isotherm in Figure 15 and equals the water activity multiplied by 100. Therefore, the water activity, corresponding to the initial moisture content of $75\ \%$ at the sorption isotherm for $50\ °C$, has to be taken. The result is $\alpha_w = 0{,}87$, so a relative humidity of $ERH = 87\ \%$. All figures are additionally presented in Table 3.

The drying temperature of $50\ °C$ has been chosen as a compromise of drying efficiency and size of the collector. One the one hand, the higher the temperature, the higher the drying rate (cf. Figure 9) and consequently the faster the drying occurs. On the other hand, a high temperature means a high amount of energy has to be provided and so, more solar collectors are needed. This leads to increased investment costs, as well. As a compromise between both, the drying temperature of $50\ °C$ has been chosen. Another advantage of this temperature is the existing sorption isotherm.

Table 3: Temperature, specific enthalpy, relative humidity and moisture content corresponding to the three points in the h, x - Diagram

	Temperature [°C]	Specific enthalpy [kJ/kg]	Relative humidity [%]	Moisture content [g/kg]
Inlet 1	25	55,5	60	11,9
After heat exchanger 2	50	81,3	15,4	11,9
After drying of fish 3	28	81,3	87	20,8

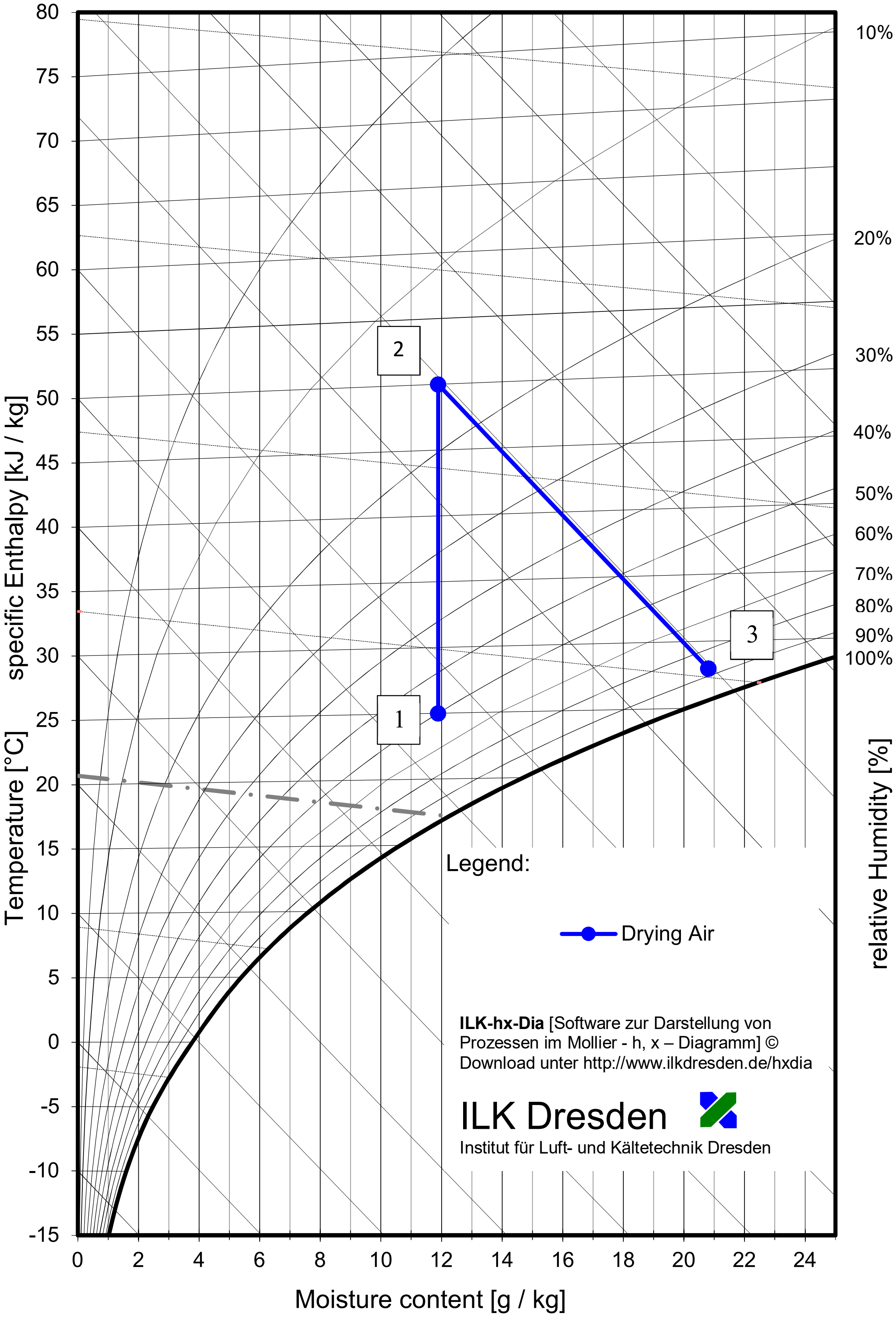

Figure 16: h, x - Diagram with charting of the drying air (1: air inlet; 2: after heat exchanger; 3: after drying of fish)

7.3. Drying time

The drying time can be estimated by the equation (3). This formula is applicable under various different conditions, if the drying-rate curve is without any sharp decreases during the falling rate period [13]. Figure 9 shows, that this is the case for the drying of sardines. The mass m_s is the one of the dry material and can be calculated by subtracting the water content from the total mass of fish $m_F = 35\ kg$ (cf. equation (4)). By using the initial moisture content of the fish of $X_{F\alpha} = 0{,}75$, a dry mass of $\boldsymbol{m_s = 8,75\ kg}$ results. A is the drying area and given by the design with $A = 3{,}84\ m^2$. All values given by the design, could be taken out of the drawings in the Appendix 2, also. Due to the fact, that the drying of fish starts with the first falling rate period, without having any constant rate (cf. Figure 5), the constant-rate period drying rate R_c equals the one of the start of the drying. The calculation can be done by equation (5). The needed moisture contents are the initial one ($X_{F\alpha}$), the final one ($X_{F\omega}$) and the first critical one (X_{Fc}) of the fish. The critical moisture content is the one, when the constant-rate period ends, and the falling rate starts, so in this case the initial moisture content of $X_{Fc} = 0{,}75$.

$$t_d = \frac{m_s}{A * R_c} * \left(X_{F\alpha} - X_{Fc} + X_{Fc} * \ln \left(\frac{X_{Fc}}{X_{F\omega}} \right) \right) \quad (3)\ [13]$$

$$m_s = m_F * (1 - X_{F\alpha}) \quad (4)$$

$$R_c = \frac{h_y * (T - T_i)}{r_i} \quad (5)\ [13]$$

To calculate the constant-rate period drying rate, the heat-transfer coefficient between gas and surface of slap h_y is needed. This can be evaluated by equation (6). λ, as the thermal conductivity, is a substance-specific figure and can be taken out of tables. In this case the thermal conductivity for air at $50°C$ has to be taken. This is $\lambda = 0{,}02788 \frac{W}{m*K}$ [14]. The equivalent diameter D_e can be calculated by the equation (7) and the Reynolds number by equation (9). The Prandtl number is a substance-specific, as well, and is defined by formula (10).

$$h_y = 0{,}37 * Re^{0,8} * Pr^{0,33} * \frac{\lambda}{D_e} \quad (6)\ [13]$$

The hydraulic radius r_H, which is needed to calculate the equivalent diameter, is defined by formula (8). The cross-sectional area S and the perimeter in contact with fluid L_p are simplified defined by the space between two drawers. In this case is $S = 91.200\ mm^2$ and $L_p = 2110\ mm$. Consequently, the equivalent diameter results to $\boldsymbol{D_e = 0,173\ m^2}$**.**

$$D_e = 4 * r_H \tag{7) [13}$$

$$r_H = \frac{S}{L_p} \tag{8) [13}$$

The Reynold number is a dimensionless number for the stream. To calculate Re, the velocity of air w, the equivalent diameter D_e, the density of the fluid ρ_F and the viscosity η of the fluid are needed (cf. equation (9)). The density and the viscosity are taken simplified of air at the temperature of $50°C$, especially because the humidity is changing during the process and therefore the density and viscosity, as well. They are assumed as follows: $\rho_F = 1{,}078 \frac{kg}{m^3}$ [14] and $\eta = 19{,}67 * 10^{-6} \frac{kg}{m*s}$ [14]. The velocity can be taken as $w = 0{,}1 \frac{m}{s}$ and the equivalent diameter equals the already calculated one with equation (7). Therefore, for the Reynolds number results $\boldsymbol{Re = 948}$.

$$Re = \frac{w * D_e * \rho_F}{\eta} \tag{9}$$

The Prandtl number, as a substance-specific value, can be calculated completely out of substance properties of the fluid. So, in this case for air at the temperature of $50°C$ and pressure of 1 bar. Again, like already mentioned, the humidity gets neglected. How the Prandtl number has to be calculated, can be seen below in equation (10). There, c_p is the specific heat at constant pressure and is $c_p = 1{,}008 \frac{kJ}{kg*K}$ [14], whereby the Prandtl number is $\boldsymbol{Pr = 0,711}$.

$$Pr = \frac{c_p * \eta}{\lambda} \tag{10}$$

Out of the Reynolds number, the Prandtl number, the thermal conductivity and the equivalent diameter, the heat-transfer coefficient h_y can be calculated to $\boldsymbol{h_y = 12{,}828\frac{W}{K}}$ (cf. equation (6)).

To calculate the drying rate R_c, besides the heat-transfer coefficient, the temperature difference between the drying temperature T and the interface temperature T_i and the latent heat of vaporization at the interface temperature r_i is needed. The temperature at the interface of the fish equals the wet bulb temperature, so the temperature of the air at saturation, which is $T_i \approx 26\,°C$. For the latent heat of vaporization results a value of $r_i = 2439{,}33\frac{kJ}{kg}$ [14]. By equation (5), the drying rate can now be calculated to $\boldsymbol{R_c = 0{,}000125\frac{kg}{m^2}}$.

After calculating the drying rate, the drying time can be calculated by equation (3). The result is a drying time of approximately $\boldsymbol{t_d = 6{,}1\ h}$, so about 6 hours and 5 minutes.

7.4. Flow rate

To calculate the needed air flow rate, the change of the humidity in the air has to be calculated first. Therefore, the difference between the moisture content after the heat exchanger and after the drying has to be taken. It results $\Delta X = 8{,}9\frac{g_W}{kg_A}$. By taking the invert of this, the necessary amount of fresh air per kilogram water can be calculated to $112{,}36\frac{kg_A}{kg_W}$. To obtain the absolute mass of needed dry air, this value has to be multiplied by the amount of water, which gets removed out of the fish by the drying. This can be done by using equation (11). The mass of transferred water of $\boldsymbol{m_W = 24{,}71\ kg_W}$ results. The total amount of dry air is then $m_A = 2776{,}42\ kg_A$.

$$m_W = m_F * \frac{X_{F\alpha} - X_{F\omega}}{1 - X_{F\omega}} \qquad (11)\ [2]$$

Out of the dry air mass, the volume of air V_A can be calculated by the ideal gas law (cf. equation (12)). Thereby, the gas constant is $R_m = 8{,}314\frac{kJ}{kmol*K}$, the molar mass of the air $M_A = 28{,}963\frac{kmol}{kg}$, the temperature $T = 323{,}15\ K$and the pressure $p = 10.1300\ Pa$. For the air volume results $\boldsymbol{V_A = 2424{,}77\ m^3}$.

$$V_A = \frac{m_A * R_m * T}{M_A * p} \quad (12)$$

By using the previous calculated drying time, the air flow rate can be evaluated out of the air volume by equation (13). It results $\boldsymbol{\dot{V}_A \approx 0,1\frac{m^3}{s}}$.

$$\dot{V}_A = \frac{V_A}{t_d} \quad (13)$$

8 CFD Analysis

8.1. The simulation

To run the simulation, the model has to be simplified. Little elements, like the hinges, the lever and the welding get deleted. The mash of the drawers is replaced by a solid plate. By this, the fish has been simplified. Actually, the air will go through gaps between the fish on the mesh, also. But on this way the weaknesses of the design can be obtained easier and the simulation will be simpler.

The boundary conditions for the simulation are defined by the previous calculations. At the inlet of the chamber the air flow rate is fed. The exchange of moisture cannot be simulated by the used program (Autodesk CFD 2018). As a result, it is not possible to simulate the change in temperature of the air. This air temperature is an important value for the drying process. The higher the temperature, the faster is the drying. But it is relating directly to the flow of the air. Fresh air has the highest temperature. By rising of the moisture content of the air during the drying process, the temperature is dropping. This results in the assumption, that an equal air distribution is directly related to an equal temperature distribution. So, fresh air has a higher temperature, than the air, which has already taken moisture from the fish away. If the air flows in every level in the same way, the temperature gradients will be the same, also, and, therefore, the drying will take place in each drawer in the same way and time.

Thus, the simulation with only one boundary condition, the air flow rate, is very simple.

8.2. Results

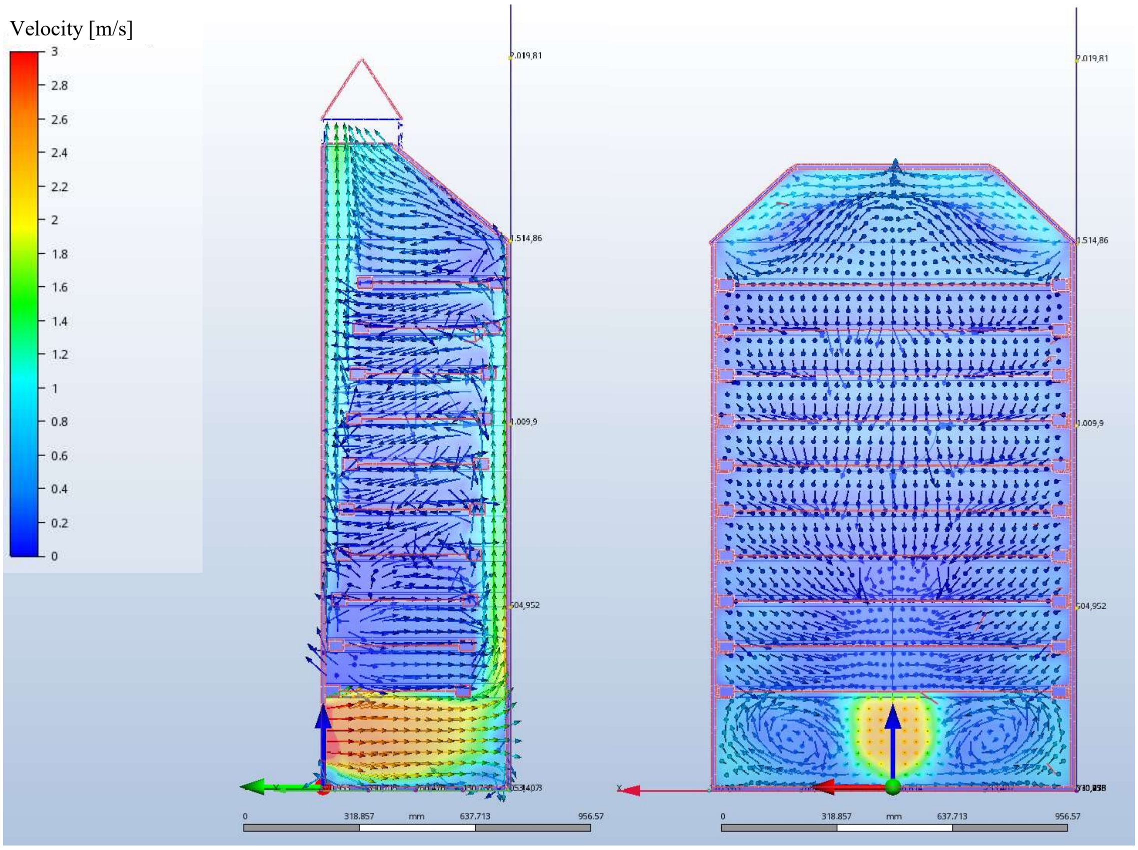

Figure 17: Cross sectional views of the CFD analysis of in the middle of the original design

Figure 17 shows the results of the CFD analysis in the middle of the device from the left side (left) and from the back (right).

The view from the left side shows that the air enters the device with a speed over 3 $\frac{m}{s}$ and slows down to approximately 1,5 $\frac{m}{s}$ before it reaches the front of the dryer. The air hits the doors and flows partly upwards. Figure 18 shows, what happen to the rest of the air. Most of it streams to the side and to the back of the device by creating a vortex. Just a small amount flows directly upwards, recognizable by the arrows in the middle of the stream directly at the doors, which are pointing up wards the device. But this air does not enter the first three levels, which can be seen in the view from the left side in Figure 17. It can be observed, that the air flows at the edges in the lower levels and streams from there

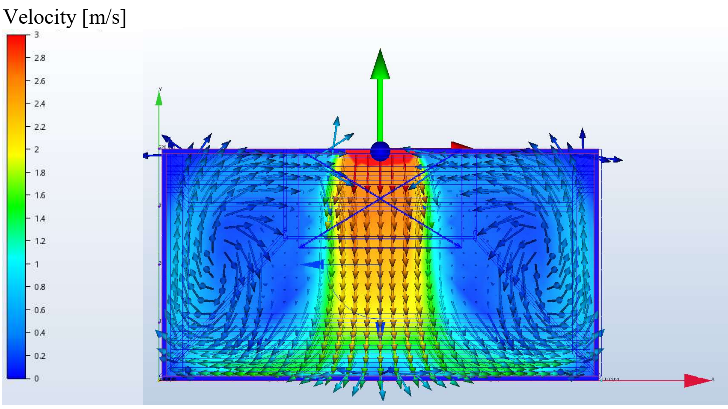

Figure 18: Top view of cross section through the air inlet

to the middle (cf. Figure 19). This leads to the phenomena, which can be observed in the cross cut from the left, that the air flows in the middle from left to right. The result of this is a vortex creation, like shown in Figure 19.

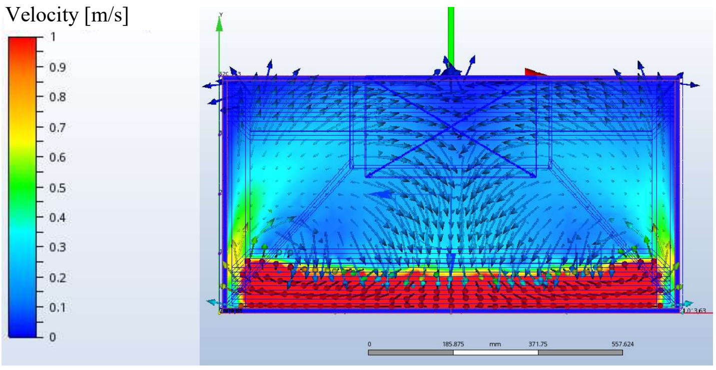

Figure 19: Cross sectional top view of the first level

Indeed, the air enters each drawer and it can be assumed, that this happens nearly simultaneously. Doubtful is, if the drying takes place simultaneously, as well. Due to the back flow of the air in the lower levels, the fish in the middle of this drawer might need more time for reaching the final moisture content, than the fish at the edges. This might happen, because the air passes first the edges, taking moisture away from the fish, before streaming through the middle, like it can be seen in the cross cut in Figure 19. This air has then a higher moisture content than the “fresh” air and cannot remove the moisture of the fish in the same way. The drying in the middle takes place later than the one at the edges.

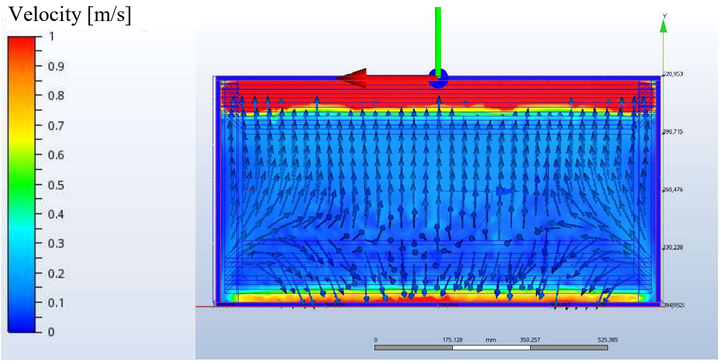

Figure 20: Cross sectional top view of the last level

The flowing of the already used air has another negative impact. It might happen, that this air enters another drawer again. This would lead to a degradation of the drying process, too. This influence will not be as big as in the levels, because a dilution of used and fresh air takes place, but still it will influence the process.

In the upper drawers, the air flows nearly straight from the doors to the back of the chamber and then upwards to the outlet at the top, like the cross cut Figure 20 shows.

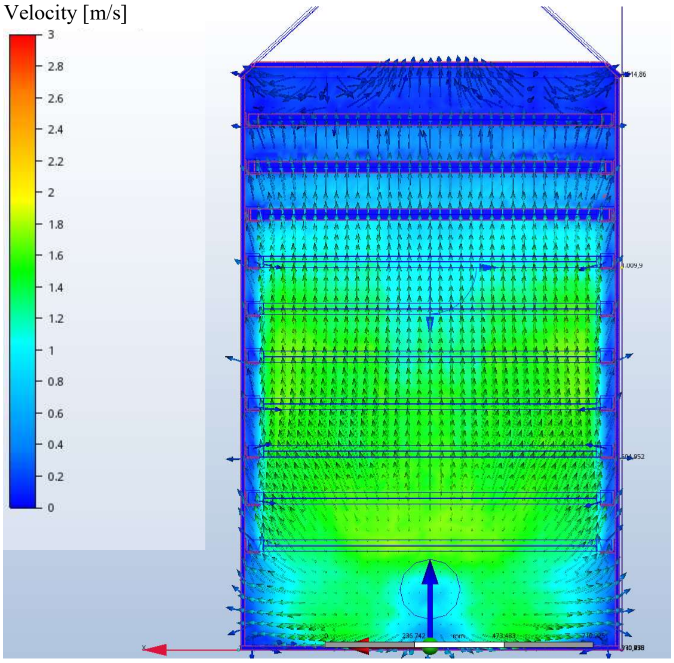

Figure 21: Cross-sectional view from the back of the front of the original design

As a result of all the cross sectional top views can be taken, that upstreaming of the air is a problem of this design. Already in Figure 18 is striking, that the air does not flow equally upwards but at the edges first to the sites. Figure 21 shows this, as well. This, in turn, causes an irregular upwards stream. The air flows at the edges not straight upwards but more to the sites. This effect begins to decrease at the third level, so at the same time, when the backflow of the air became less. Also, the air in the beginning is not distributed over the whole cross section but concentrated at the doors. Both is a result of the air inlet and leads to the fact that in the first levels the air enters at the edges and not equally along the whole drawer side. These effects getting less with the height, so that the air flows equally through the levels in the upper ones, like shown in Figure 20.

The improvements, which have to be done, are the prevention of a vortex creation in the lower levels and an upstream air movement, which is more equally and distributed in the cross section.

8.3. Improvements

8.3.1 Design

To improve the air flow and to minimize the described problems, several approaches are possible.

First, it would be possible to change the process parameters. A reduction of the air flow would lead to lower velocities and this would reduce problems like the distribution of the air. But at the same time, this would cause a reduction of the drying efficiency. This kind of solution is not practicable because of another reason, as well. At this point of development, it is not possible to say something specific about the process parameters. Like already mentioned are the previous calculations not exact but assumptions. A rise or a reduction of the air flow rate in the praxis is likely. To ensure, that the drying takes place by higher as well as lower air flow rates, the design has to be optimised. Two constructive changes have been done, to do this. The improved design is shown in Figure 22.

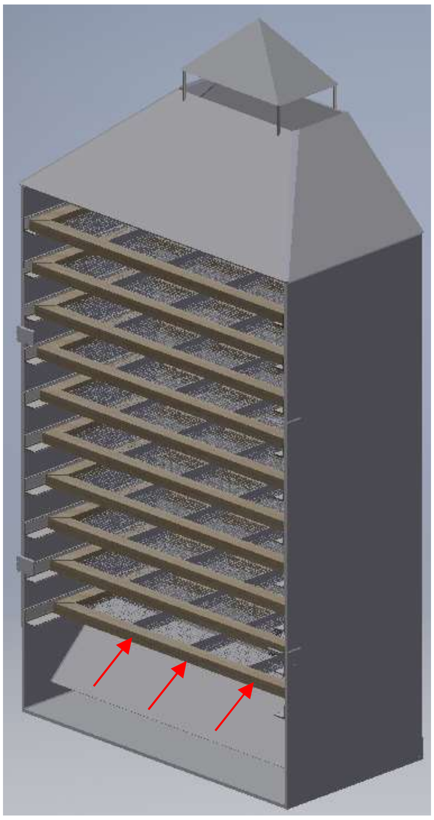

Figure 22: Isometric view of the improved drying chamber

To ensure a better distribution of the air stream, a deflection plate has been equipped (cf. Figure 23). The idea is to position the impact of the air from the doors to a plate. By an inclination of this plate, the air should be directed in the right direction. At the same time, space has been created for the equal formation of the stream, before it reaches the lowest drawer.

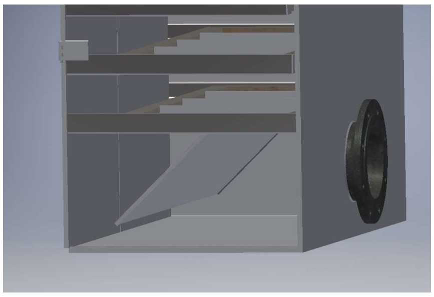

Figure 23: Detailed view of the inlet and deflection plate of the improved drying chamber

The other change is the adding of jetties inside of the drawer. They can be seen at the tray in Figure 22 (red arrows) and in detail in the drawing “Chamber” in the Appendix 2. Three of them in each tray should prevent the formation of the vortex and should channel the air in the right direction.

8.3.2 Simulation results

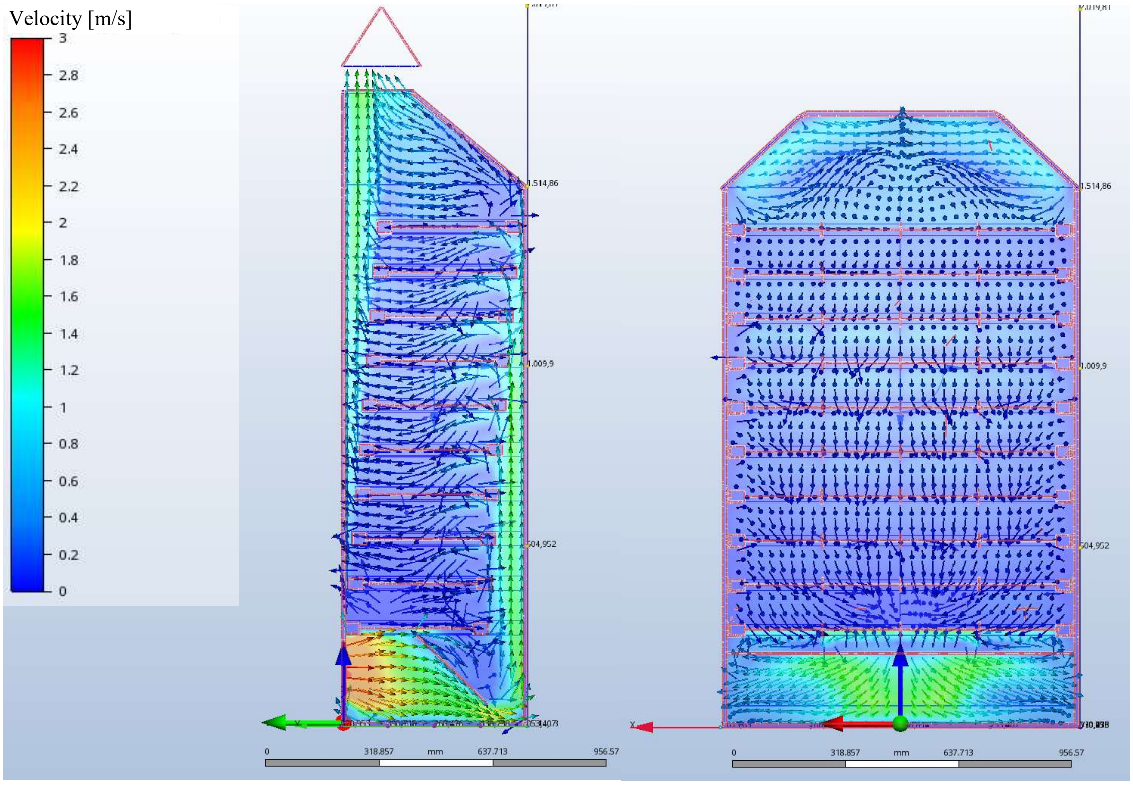

Figure 24: Cross sectional views of the CFD analysis of in the middle of the improved design

Figure 24 shows the cross-sectional views of the CFD analysis at the same position as in Figure 17, so that a direct comparison is possible. First it can be seen in the view from the back, that the backflow of the air takes place now only in the lowest boarder and not like before in the lowest three. The same is visible at the view from the left. In every level, except the lowest one, the air streams from the front to the back of the chamber. From this point of view, the influence of the deflection plate can be seen, as well. The air flows much more equal and controlled upwards. This shows Figure 25, too. Especially in comparison with Figure 21 is striking, that the air is from the beginning much more equally spread. The effect of the to the edges flowing air is much less and therefore, the equally spread air can be observed already at the first drawer.

The jetties, which has been added to the drawers, are reducing the backflow, as well. In Figure 26 are shown cross-sectional top views of the first and second drawer. It can be seen, that in the left picture of the first level, the air flow goes on the right and left side nearly straight. The vortex, as in Figure 19, has disappeared nearly. Indeed, the air is streaming back in the middle of the drawer but not anymore at the edges. By taking a look to the second level (right picture), no vortex can be observed. Noticeable is the backstream in the entry of both levels. This happens, because the air enters the drawer in the top and flows then down and back. But this happens only with a small amount of the air, most of it streams forward to the back of the chamber. This phenomenon can be observed in the view from the left in Figure 24, as well. It takes place in each level. But this should not have a great impact to the drying process, because by passing the fish the air is still “fresh” and the influence of the backflow is not big, due to the small amount of air.

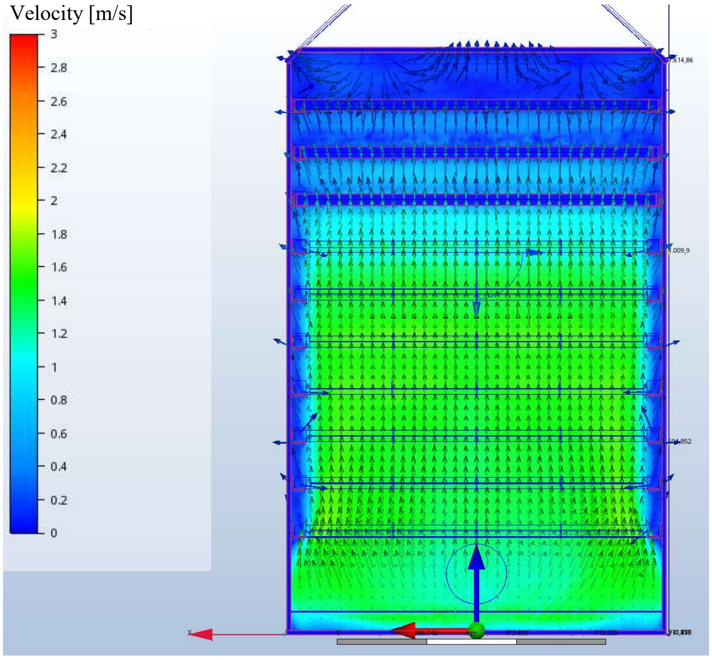

Figure 25: Cross-sectional view from the back of the front of the improved design

The velocities of the air by passing the drawers can be observed the best way in Figure 26. Due to the colour can be assumed that the air velocity is about 0,1 $\frac{m}{s}$. Nearly the same can be observed for the original design (cf. Figure 19, Figure 20) but there the velocity profile is much more irregular, because of the more irregular air flow. The equal velocity is important for the equal drying. The value of 0,1 $\frac{m}{s}$ confirms the previous assumption of the calculation of the Reynolds number for the drying time.

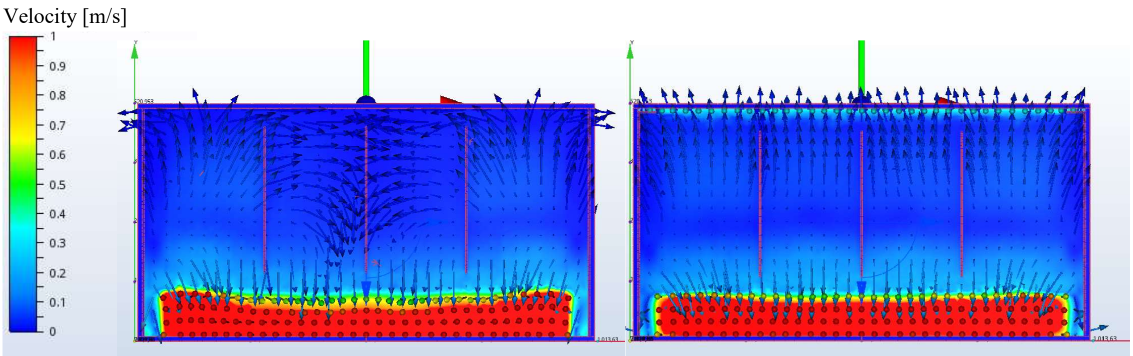

Figure 26:Cross-sectional top view of the first (left) and second (right) level of the improved design

8.4. Air flow Evaluation

The air flow of the improved design has nearly in each level an equal streaming from the front to the back of the chamber. Only in the first level can be observed a partly backflow in the middle of the drawer. The velocities are in each level about the same, as well. It can be assumed, that the drying process takes place equally inside of the whole chamber.

9 Design Evaluation

The design itself is as simply as possible. No special parts or difficult constellation are included. The whole chamber can be assembled by welding, which makes the device at the same time very stable. The size of the chamber is big enough for a high capacity but at the same time small enough, that one person can use it without problems. So, the trays have the size, which can be handled of one person on his own.

The needed air flow rate will be delivered by a fan, which is attached at the flange at the inlet. This one has a standardized size of DN 150, so that the attaching of other parts can be done easily.

The outlet of the air is remaining at the top of the chamber as a kind of chimney.

Much maintenance is not needed. Only important is, to clean the trays after each usage, to prevent any kind of spoiling of the food. Nevertheless, spoiling of the fish by microorganisms or bacteria, due to inadequate cleaning, is not likely, because of the running temperatures and the removing of the water out of the fish.

10 Conclusion

The improved final design fulfils the set criteria. The simulation of the air flow has been optimized, so that the drying will take place as equally as possible. The design itself is still simple and much maintenance is not needed. The costs for assembling this device will not be too high, because of this simplicity of the design and the used parts. Thus, the chance, that the drying of the fish by this device is economical even for small villages, is high.

The calculations have shown, that the drying process can take place most of the year in one day. If the drying process needs about $6\ h$, about $182{,}5\ h$ of sun each moth is necessary. Figure 11 shows, that this amount of sun hours is available nearly the whole year. Nevertheless, the calculations are not total reliable, due to several assumptions, which have been done, but are giving a good first impression.

Further testing is still needed. It would be useful to build a new prototype and to test it next. It is necessary to check the calculations. Many assumptions have been done in the first place, so figures like drying time and air flow rate has to be examined further. The capacity is another factor, which has to be tested further. The drying takes place most efficiently, if each tray is loaded with a single layer of fish. If the number of 10 trays is enough, cannot be said for sure, but a change in the number of levels can be done easily by this kind of design.

In general, this kind of device has a positive impact for the African fishers. The drying chamber has several advantages in comparison to the current used open-air sun drying. The losses by moulding and natural influences, like rain or animals, will decrease. At the same time the product is healthier by saving of vitamins due to the indirect drying. Workload can be saved as well, because a supervision of the drying process all the time, like it was necessary by the open-air sun drying, is not needed. Of course, the investment cost of the chamber is higher, than the traditional way of drying. But the savings by this kind of device might be big enough to make this investment worth it.

Finally, it can be said, that the in this thesis developed design is a good base for further developing of an economical working fish dryer for small scale drying in Africa.

References

[1] M. Kraume, Transportvorgänge in der Verfahrenstechnik - Grundlagen und apparative Umsetzung, Berlin: Springer, 2012.

[2] O. Prakash and A. Kumar, Solar Drying Technology - Concept, Design, Testing, Modelling, Economics, and Environment, Singapore: Springer, 2017.

[3] V. Belessiotis and E. Delyannis, "Solar drying," *Solar Energy,* vol. 85, no. 8, pp. 1665-1691, 2011.

[4] M. Toujani, L. Hassini, S. Azzouz and A. Belighith, "Drying characteristics and sorption isotherms of silverside fish (Atherina)," *International Journal of Food Science & Technology ,* vol. 46, no. 3, pp. 594 - 600, 2011.

[5] M. C. Augustus Leon, S. Kumar and S. Bhattacharya, "A comprehensive procedure for performance of solar food dryers," *Renewable & Sustainable Energy Reviews,* vol. 6, no. 4, pp. 367-393, 2002.

[6] M. Lixandru, "Properties and Benefits of Sardines," Nature Word, 19 December 2017. [Online]. Available: https://www.natureword.com/properties-and-benefits-of-sardines/. [Accessed 17 February 2018].

[7] L. A. Ogonda, E. K. Muge, F. J. Mulaa and B. N. Mbatia, "Proximate composition of Rastrineobola argentea (Dagaa) of Lake Victoria-Kenya," *African Journal of Biochemistry Research,* vol. 8, no. 1, pp. 1-6, 2014.

[8] H. Suzuki, S. Hayakawa, S. Wada, E. Okazaki and M. Yamazawa, "Effect of Solar Drying on Vitamin D3 and Provitamin D3 Contents in Fish Meat," *Journal of Agricultural and Food Chemistry,* vol. 36, no. 4, pp. 803-806, 1988.

[9] B. Hadrich, N. Boudhrioua and N. Kechaou, "Drying of Tunisian sardine (Sardinella aurita) experimental study and three-dimensionla transfer modeling of drying kinetics," *Journal of Food Engineering,* vol. 84, no. 1, pp. 92-100, 2008.

[10] World Weather & Climate Information, "Climate Kisumu," 2016. [Online]. Available: https://weather-and-climate.com/average-monthly-Rainfall-Temperature-Sunshine,kisumu-ke,Kenya. [Accessed 27 February 2018].

[11] L. Symington, "Fish dehydrated with solar energy at Bao Beach, Kenya," GoSol, 28 August 2017. [Online]. Available: https://www.gosol.org/solar-fish-dehydrating-bao-beach. [Accessed 19 March 2018].

[12] U. Fischer, R. Gomeringer, M. Heinzler, R. Kilgus, F. Näher, S. Oesterle, H. Paetzold and A. Stephan, Tabellenbuch Metall, 45. Auflage, Haan-Gruiten: Europa-Lehrmittel, 2011.

[13] W. L. McCabe, J. C. Smith and P. Harriott, Unit Operations of Chemical Engineering Seventh Edition, New York: McGraw-Hill Higher Education, 2005.

[14] P. D.-I. P. Stephan, VDI-Wärmeatlas, 11. Auflage, Düsselorf: VDI-Gesellschaft Verrfahrenstechnik und Chemieingeneurswesen (GVC), 2013.

[15] Conde Nast, “Fish, sardine, Atlantic, canned in oil, drained solids with bone Nutrition Facts & Calories,” SELFNutrition Data, [Online]. Available: http://nutritiondata.self.com/facts/finfish-and-shellfish-products/4114/2#. [Accessed 17 February 2018].

[16] J. Banout, P. Ehl, J. Havlik, B. Lojka, Z. Polesny and V. Verner, “Design and performance evaluation of a double-pass solar dryer for drying of red chilli (Capsicum annum L.),” *Solar Energy,* vol. 85, no. 3, pp. 506-515, 2011.

APPENDICES

Appendix 1. Nutrition Information for 100g for sardine, Atlantic, canned in oil, drained solids with bone **[15]**

1 (2)

NUTRITION INFORMATION

Amounts per 100 grams

Calorie Information

Amounts Per Selected Serving		%DV
Calories	208 (871 kJ)	10%
From Carbohydrate	0.0 (0.0 kJ)	
From Fat	103 (431 kJ)	
From Protein	105 (440 kJ)	
From Alcohol	0.0 (0.0 kJ)	

Carbohydrates

Amounts Per Selected Serving		%DV
Total Carbohydrate	0.0 g	0%
Dietary Fiber	0.0 g	0%
Starch	0.0 g	
Sugars	0.0 g	

More details

Fats & Fatty Acids

Amounts Per Selected Serving		%DV
Total Fat	11.5 g	18%
Saturated Fat	1.5 g	8%
Monounsaturated Fat	3.9 g	
Polyunsaturated Fat	5.1 g	
Total trans fatty acids	~	
Total trans-monoenoic fatty acids	~	
Total trans-polyenoic fatty acids	~	
Total Omega-3 fatty acids	1480 mg	
Total Omega-6 fatty acids	3544 mg	

Learn more about these fatty acids and their equivalent names

More details

Protein & Amino Acids

Amounts Per Selected Serving		%DV
Protein	24.6 g	49%

More details

Vitamins

Amounts Per Selected Serving		%DV
Vitamin A	108 IU	2%
Vitamin C	0.0 mg	0%
Vitamin D	272 IU	68%
Vitamin E (Alpha Tocopherol)	2.0 mg	10%
Vitamin K	2.6 mcg	3%
Thiamin	0.1 mg	5%
Riboflavin	0.2 mg	13%
Niacin	5.2 mg	26%
Vitamin B6	0.2 mg	8%
Folate	12.0 mcg	3%
Vitamin B12	8.9 mcg	149%
Pantothenic Acid	0.6 mg	6%
Choline	85.0 mg	
Betaine	~	

More details

Minerals

Amounts Per Selected Serving		%DV
Calcium	382 mg	38%
Iron	2.9 mg	16%
Magnesium	39.0 mg	10%
Phosphorus	490 mg	49%
Potassium	397 mg	11%
Sodium	505 mg	21%
Zinc	1.3 mg	9%
Copper	0.2 mg	9%
Manganese	0.1 mg	5%
Selenium	52.7 mcg	75%
Fluoride	~	

2 (2)

Sterols

Amounts Per Selected Serving		%DV
Cholesterol	142 mg	47%
Phytosterols	~	

More details

Other

Amounts Per Selected Serving		%DV
Alcohol	0.0 g	
Water	59.6 g	
Ash	3.4 g	
Caffeine	0.0 mg	
Theobromine	0.0 mg	

Footnotes for Fish, sardine, Atlantic, canned in oil, drained solids with bone

Source: Nutrient data for this listing was provided by USDA SR-21. Each "~" indicates a missing or incomplete value.

Percent Daily Values (%DV) are for adults or children aged 4 or older, and are based on a 2,000 calorie reference diet. Your daily values may be higher or lower based on your individual needs.

Appendix 2. Assembly Drawing of the Drying Chamber

(1) Wall Back
(2) Wall Side
(3) Bottom Plate
(4) Door left
(5) Door right
(6) Roof front
(7) Roof side
(8) Capping
(9) Capping front
(10) Capping side
(11) Drawer
(12) Drawer frame front
(13) Drawer frame side
(14) Bulkhead
(15) Stopper Drawer
(16) Arm
(17) Stopper Arm
(18) Deflecting Plate
(19) Drying Chamber

6 5 4 3 2 1

D C B A

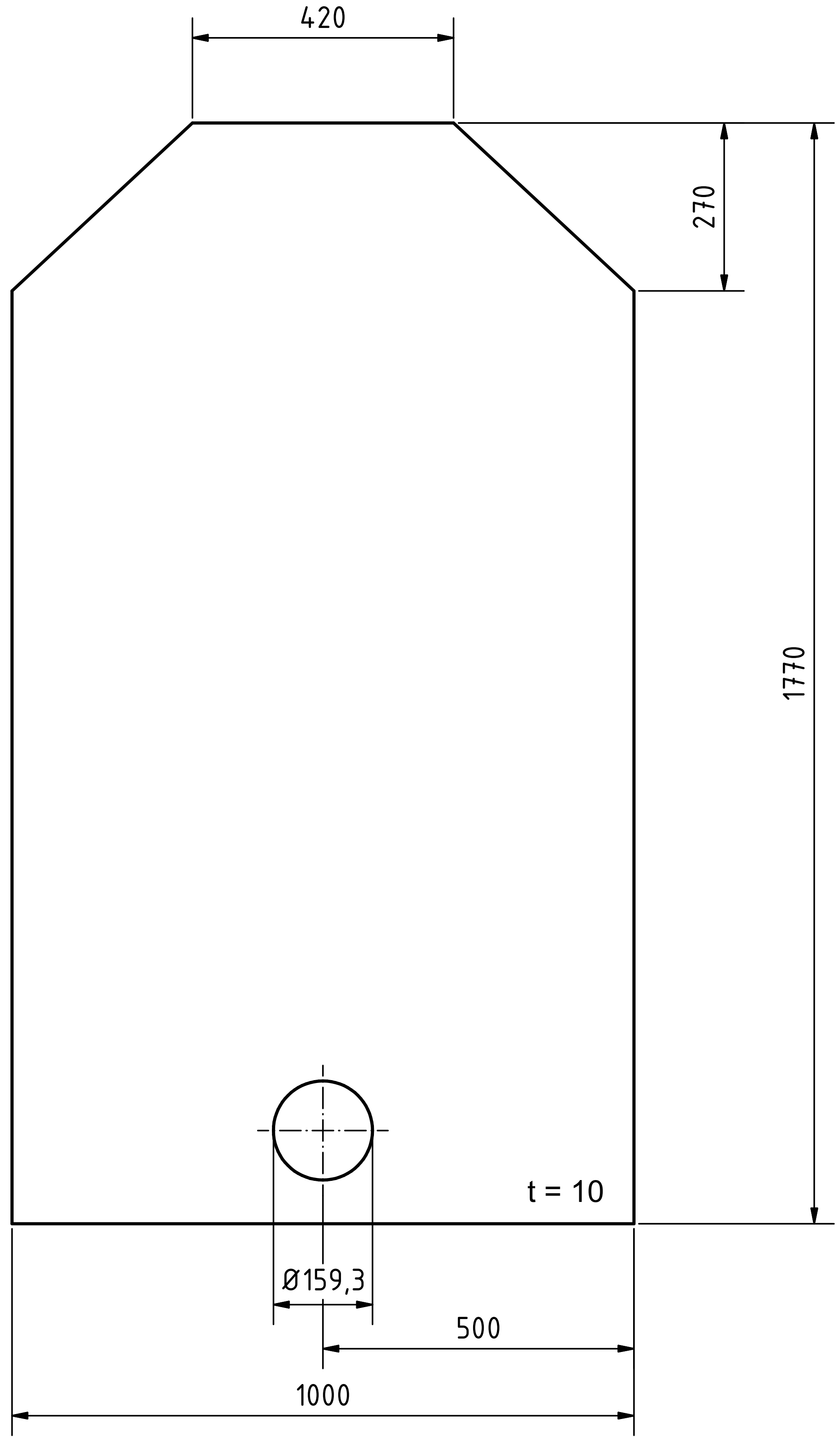

Rz 63 (✓)

General tolerance according to DIN ISO 2768 - mK		Scale 1:10	Material X8CrNiS18-9 (1.4305)
		Drying Chamber	
	Date	Name	
Author	16.04.2018	L. Büscher	Wall Back
Checked			
Approved			
HOCHSCHULE HANNOVER UNIVERSITY OF APPLIED SCIENCES AND ARTS	TAMPERE UNIVERSITY OF APPLIED SCIENCES		1
			A3

Status	Changes	Date	Name

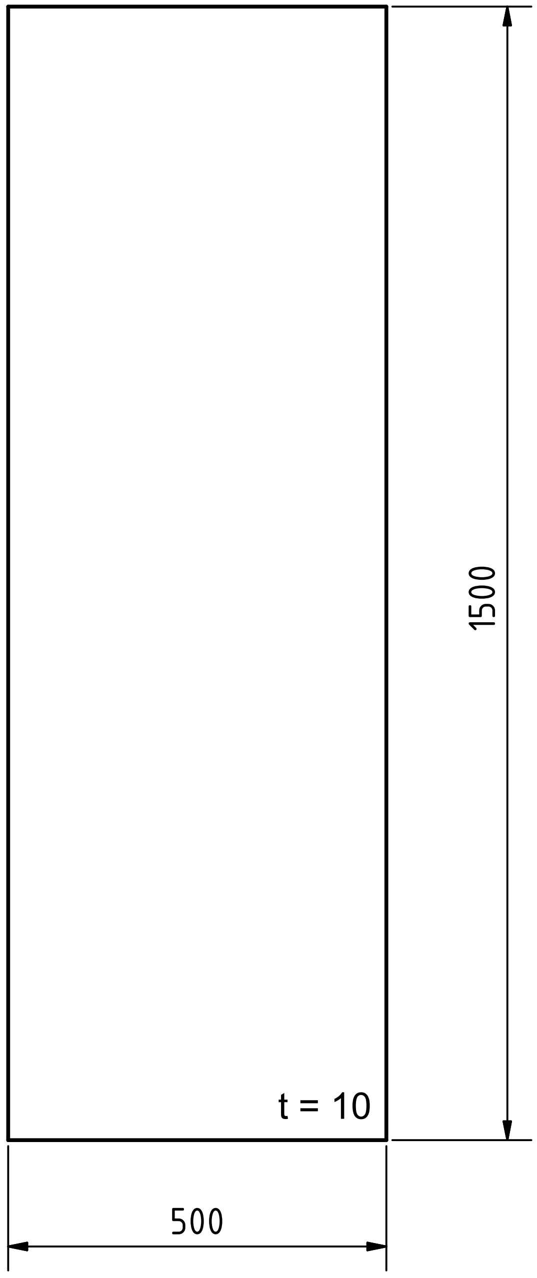

2 x

Rz 63

General tolerance according to DIN ISO 2768 - mK

Scale	1:10	Material	X8CrNiS18-9 (1.4305)

Drying Chamber

	Date	Name
Author	16.04.2018	L. Büscher
Checked		
Approved		

Wall Side

HOCHSCHULE HANNOVER UNIVERSITY OF APPLIED SCIENCES AND ARTS

TAMPERE UNIVERSITY OF APPLIED SCIENCES

1

A4

Status	Changes	Date	Name

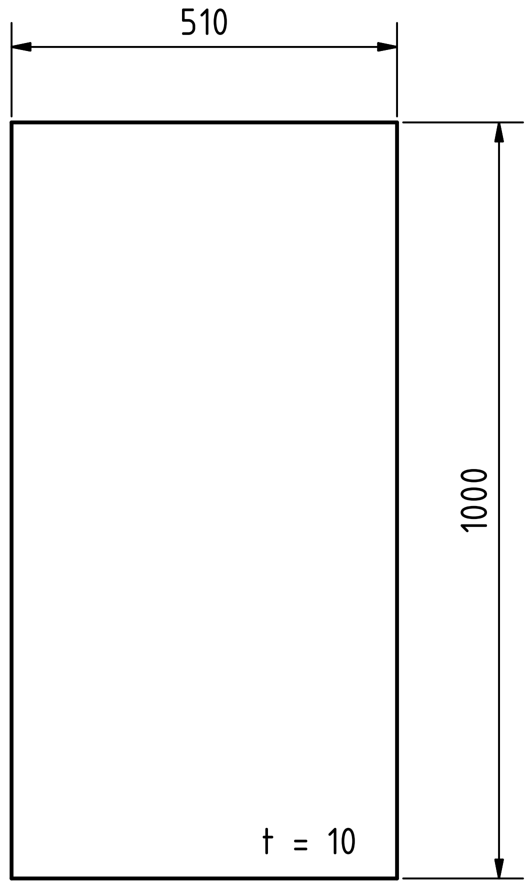

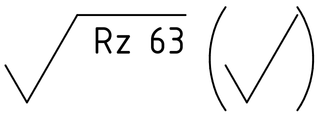

General tolerance according to DIN ISO 2768 - mK

Scale 1:10

Material X8CrNiS18-9 (1.4305)

Drying Chamber

	Date	Name
Author	16.04.2018	L. Büscher
Checked		
Approved		

Base Plate

HOCHSCHULE HANNOVER UNIVERSITY OF APPLIED SCIENCES AND ARTS

TAMPERE UNIVERSITY OF APPLIED SCIENCES

1

A4

Status	Changes	Date	Name

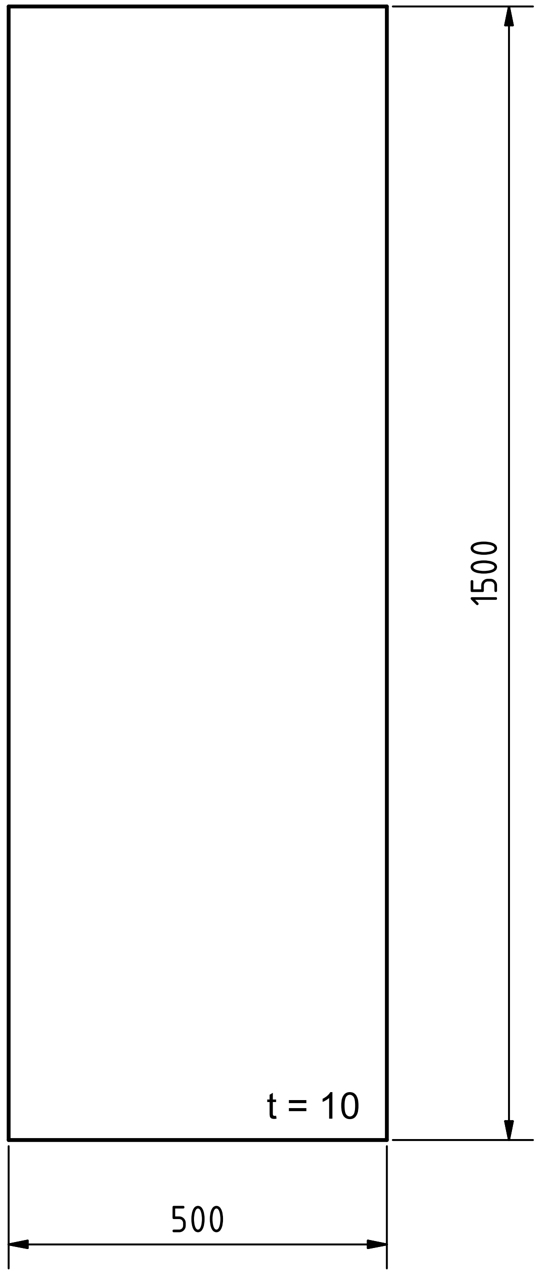

Rz 63

General tolerance according to DIN ISO 2768 - mK		Scale 1:10	Material X8CrNiS18-9 (1.4305)
		Drying Chamber	
	Date	Name	
Author	16.04.2018	L. Büscher	Door left
Checked			
Approved			
HOCHSCHULE HANNOVER UNIVERSITY OF APPLIED SCIENCES AND ARTS	TAMK TAMPERE UNIVERSITY OF APPLIED SCIENCES		1
			A4

Status	Changes	Date	Name

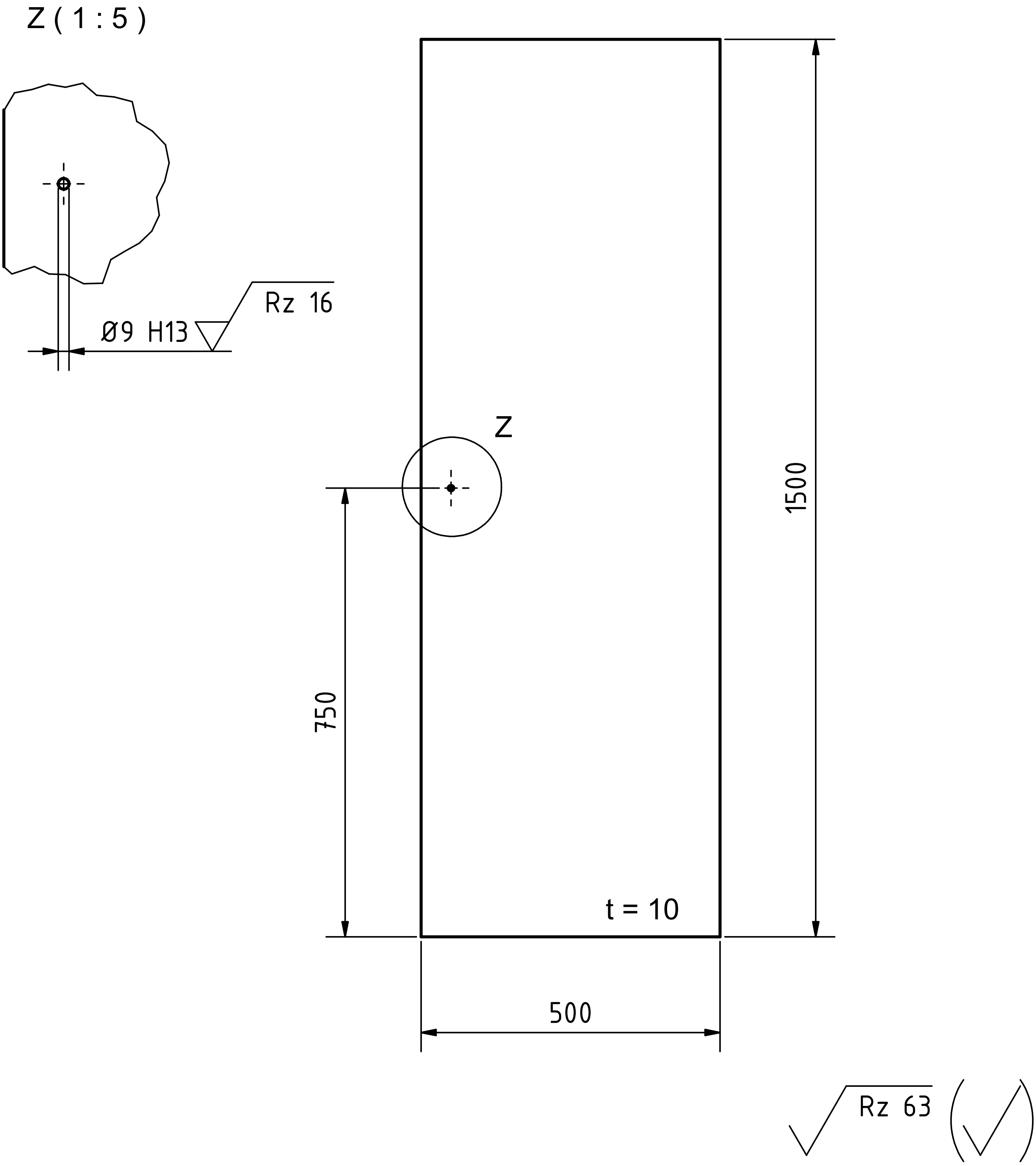

General tolerance according to DIN ISO 2768 - mK			Scale 1:10	Material	X8CrNiS18-9 (1.4305)
			Drying Chamber		
	Date	Name	Door right		
Author	16.04.2018	L. Büscher			
Checked					
Approved					
HOCHSCHULE HANNOVER UNIVERSITY OF APPLIED SCIENCES AND ARTS	TAMPERE UNIVERSITY OF APPLIED SCIENCES			1	
				A4	

Status	Changes	Date	Name

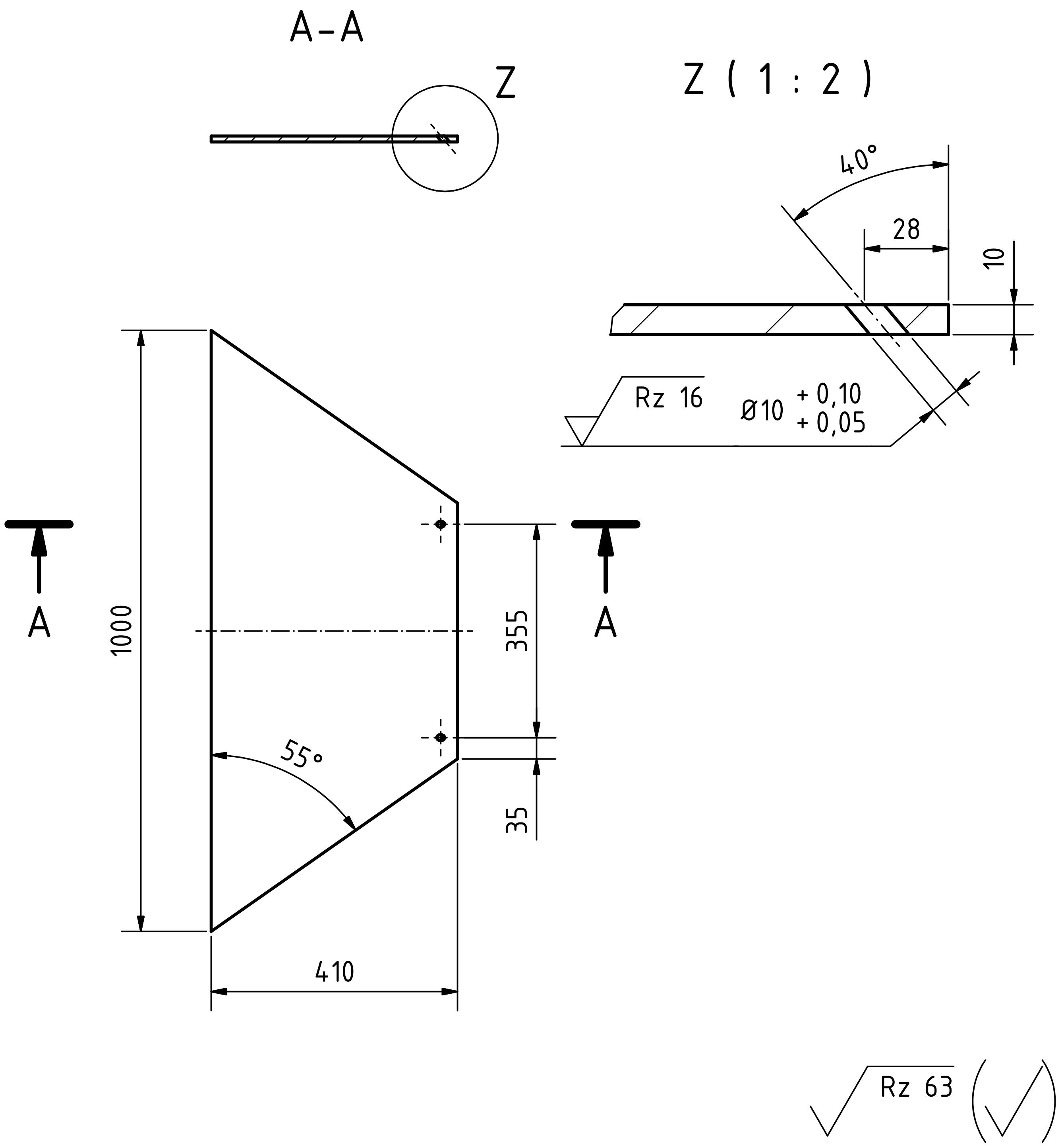

General tolerance according to DIN ISO 2768 - mK	Scale 1:10	Material X8CrNiS18-9 (1.4305)
	Drying Chamber	

	Date	Name
Author	16.04.2018	L. Büscher
Checked		
Approved		

Roof front

Status	Changes	Date	Name

HOCHSCHULE HANNOVER UNIVERSITY OF APPLIED SCIENCES AND ARTS

TAMK TAMPERE UNIVERSITY OF APPLIED SCIENCES

1

A4

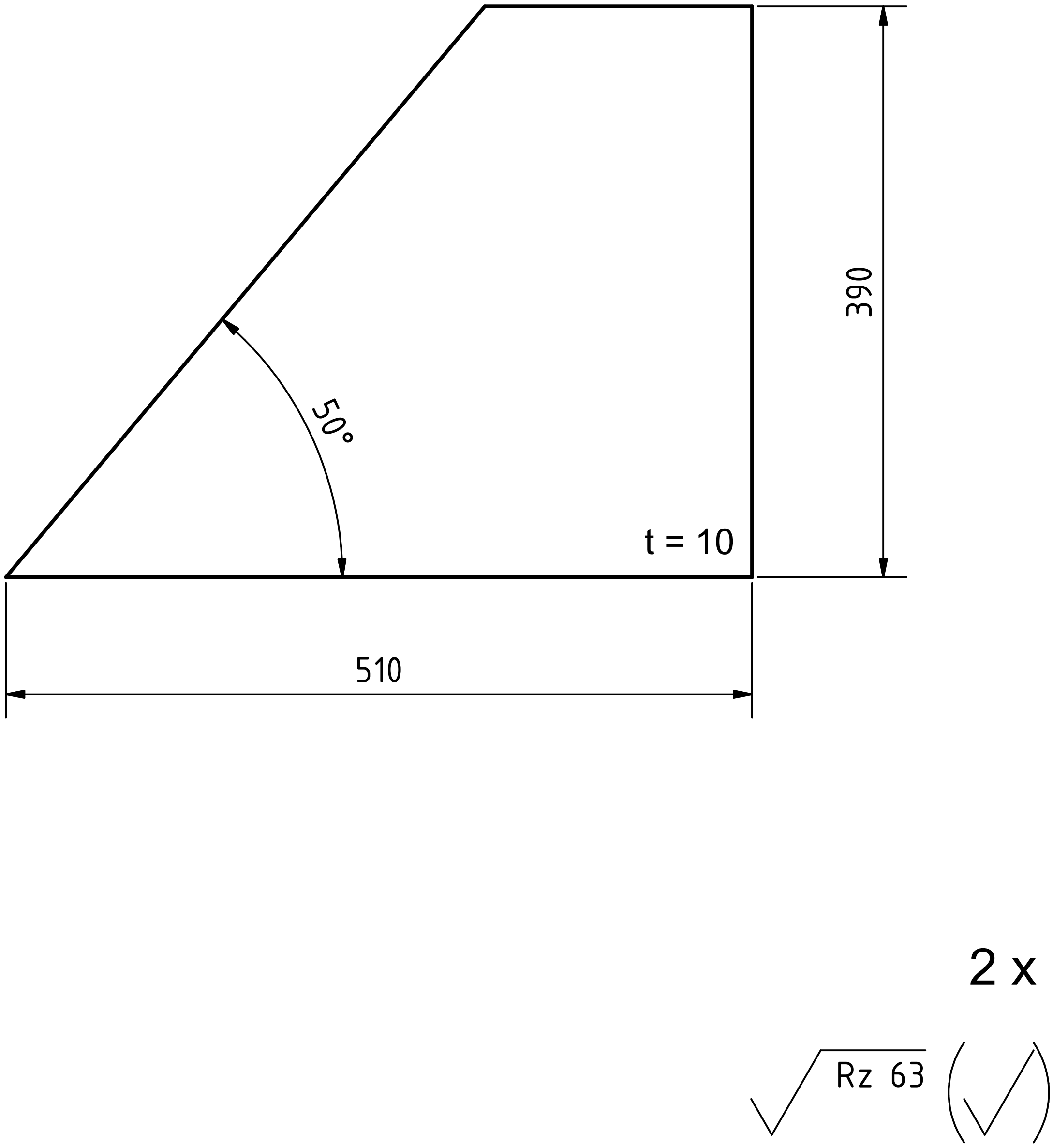

General tolerance according to DIN ISO 2768 - mK		Scale 1:10	Material X8CrNiS18-9 (1.4305)
		Drying Chamber	

	Date	Name
Author	16.04.2018	L. Büscher
Checked		
Approved		

Roof side

HOCHSCHULE HANNOVER UNIVERSITY OF APPLIED SCIENCES AND ARTS

TAMPERE UNIVERSITY OF APPLIED SCIENCES

Status	Changes	Date	Name

1

A4

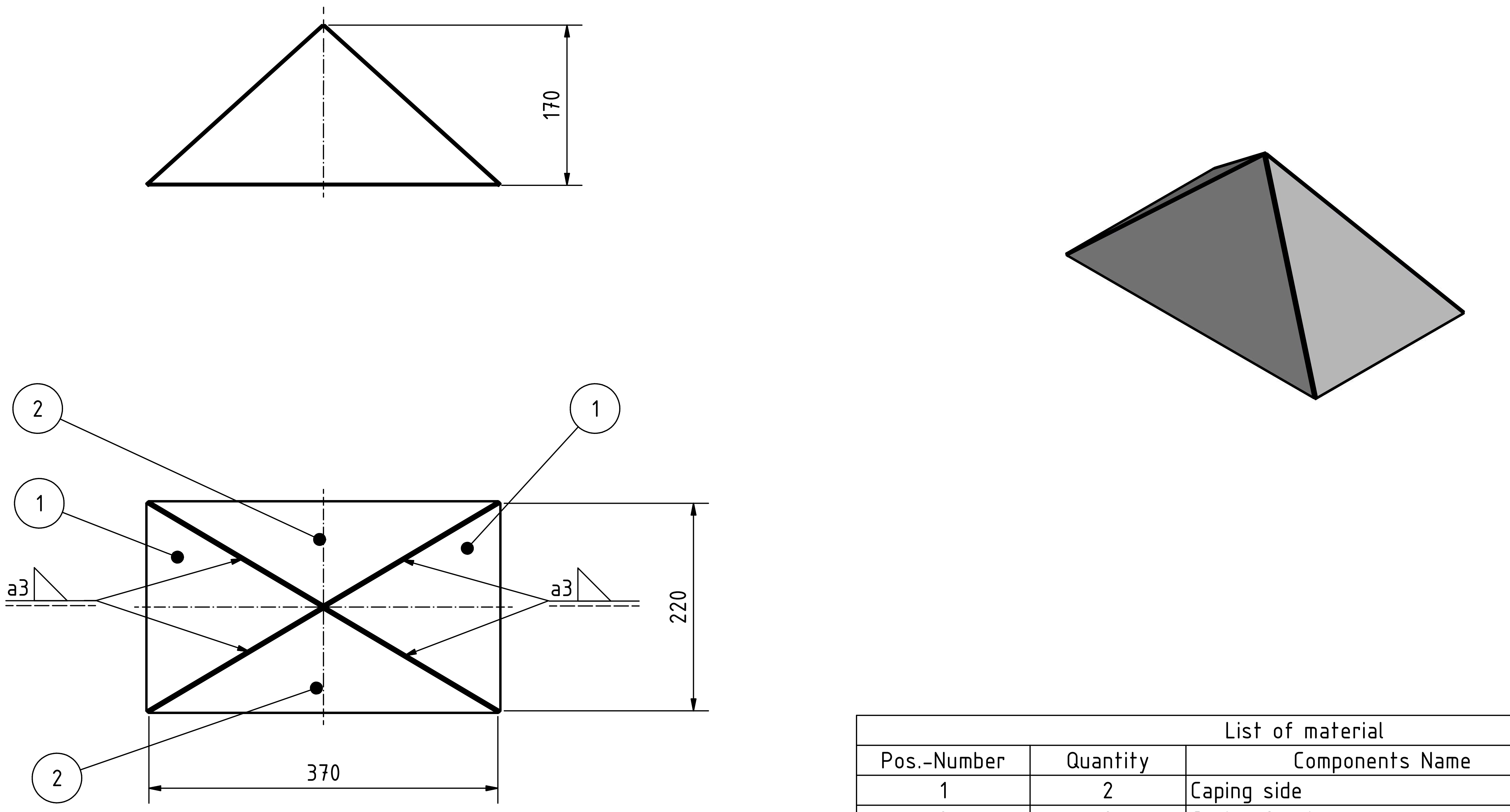

List of material			
Pos.-Number	Quantity	Components Name	Details
1	2	Caping side	
2	2	Caping front	

General tolerance according to DIN ISO 2768 - mK

Scale 1:10

Drying Chamber

	Date	Name
Author	19.04.2018	L. Büscher
Checked		
Approved		

Caping

1

A3

Status | Changes | Date | Name

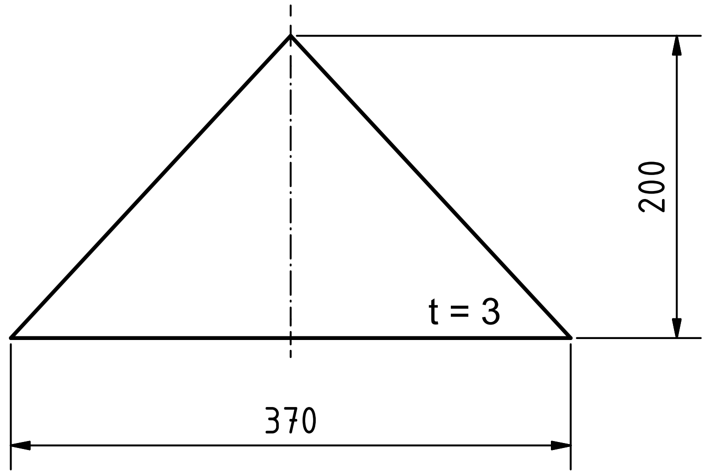

2 x

Rz 63

General tolerance according to DIN ISO 2768 - mK		Scale 1:5	Material X8CrNiS18-9 (1.4305)
		Drying Chamber	

	Date	Name
Author	19.04.2018	L. Büscher
Checked		
Approved		

Caping front

HOCHSCHULE HANNOVER UNIVERSITY OF APPLIED SCIENCES AND ARTS

TAMPERE UNIVERSITY OF APPLIED SCIENCES

1

A4

Status	Changes	Date	Name

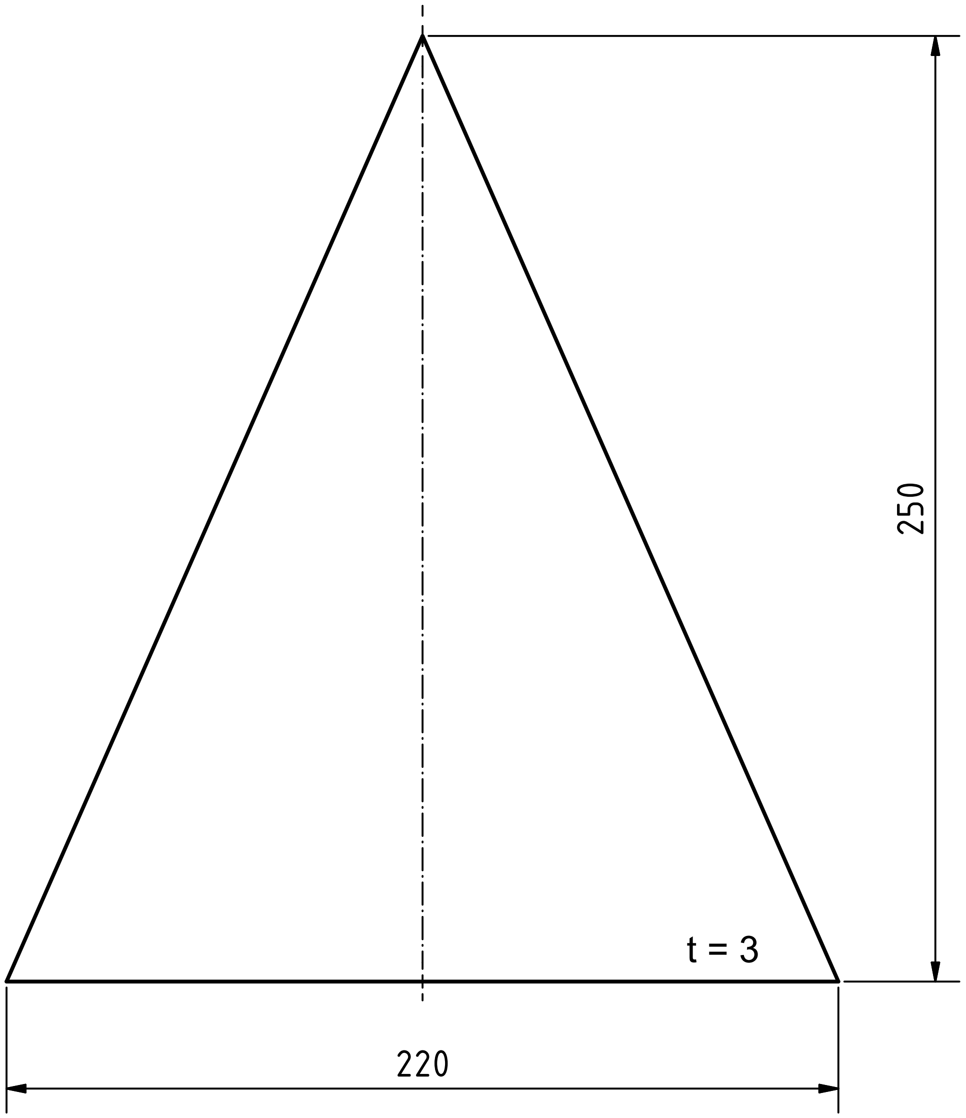

2 x

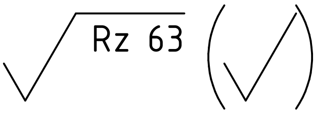

General tolerance according to DIN ISO 2768 - mK	Scale 1:2	Material X8CrNiS18-9 (1.4305)
	Drying Chamber	

	Date	Name
Author	19.04.2018	L. Büscher
Checked		
Approved		

Caping side

Hochschule Hannover University of Applied Sciences and Arts — TAMK Tampere University of Applied Sciences

1

A4

Status	Changes	Date	Name

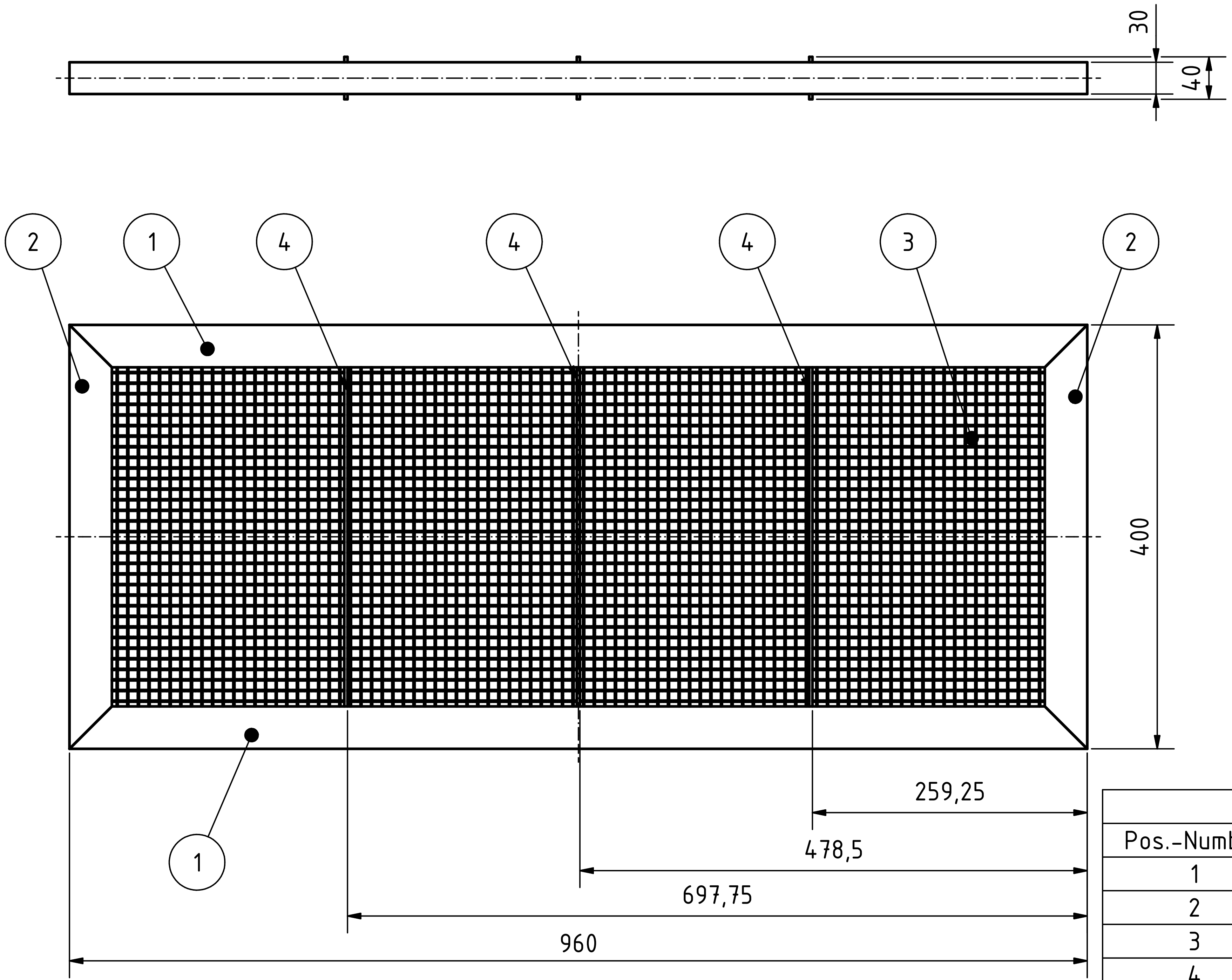

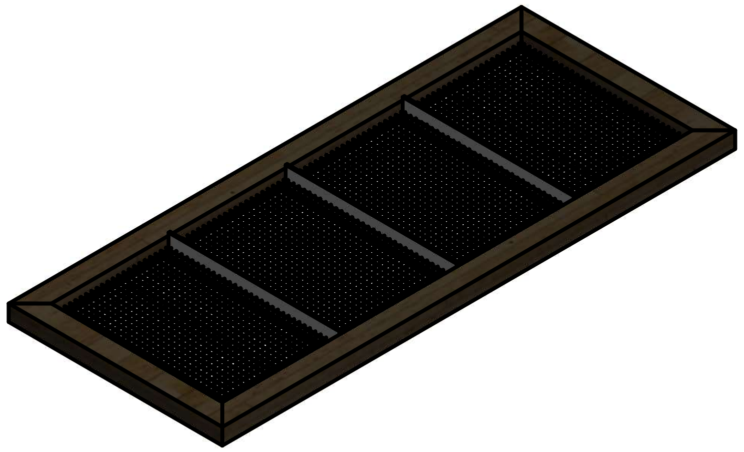

10 x

List of Material

Pos.-Number	Quantity	Components Name	Details
1	2	Drawer Frame front	
2	2	Drawer Frame side	
3	1	Mesh	
4	3	Bulkhead	

General tolerance according to DIN ISO 2768 - mK

Scale 1:5

Drying Chamber

	Date	Name
Author	20.04.2018	L. Büscher
Checked		
Approved		

Drawer

1

A3

Status	Changes	Date	Name

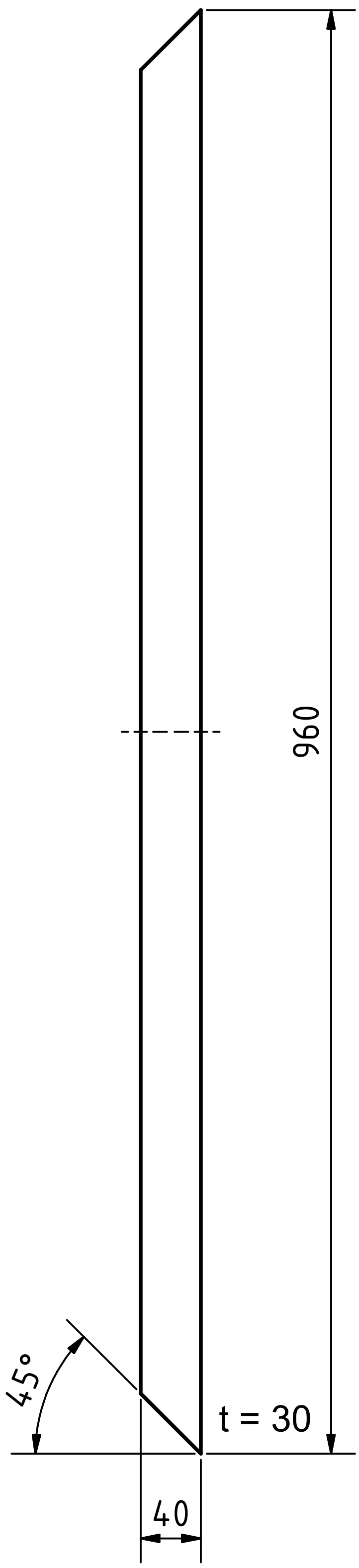

2 x for one drawer

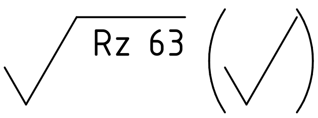

General tolerance according to
DIN ISO 2768 - mK

Scale 1:5

Material Wood

Drying Chamber

	Date	Name
Author	20.04.2018	L. Büscher
Checked		
Approved		

Drawer Frame front

Status	Changes	Date	Name

HOCHSCHULE HANNOVER
UNIVERSITY OF APPLIED SCIENCES AND ARTS

TAMPERE UNIVERSITY OF APPLIED SCIENCES

1

A4

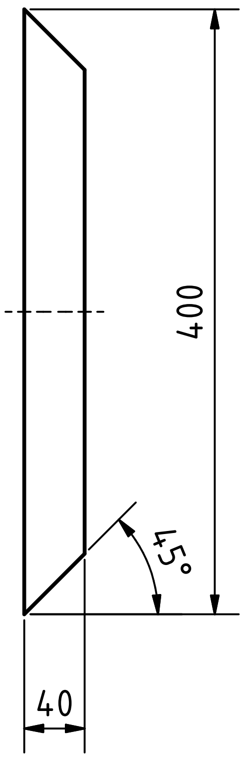

t = 30

2 x for one drawer

Rz 63

General tolerance according to DIN ISO 2768 - mK

Scale	1:5	
Material	Wood	
Drying Chamber		
	Date	Name
Author	20.04.2018	L. Büscher
Checked		
Approved		

Drawer Frame side

HOCHSCHULE HANNOVER UNIVERSITY OF APPLIED SCIENCES AND ARTS

TAMPERE UNIVERSITY OF APPLIED SCIENCES

1

A4

Status	Changes	Date	Name

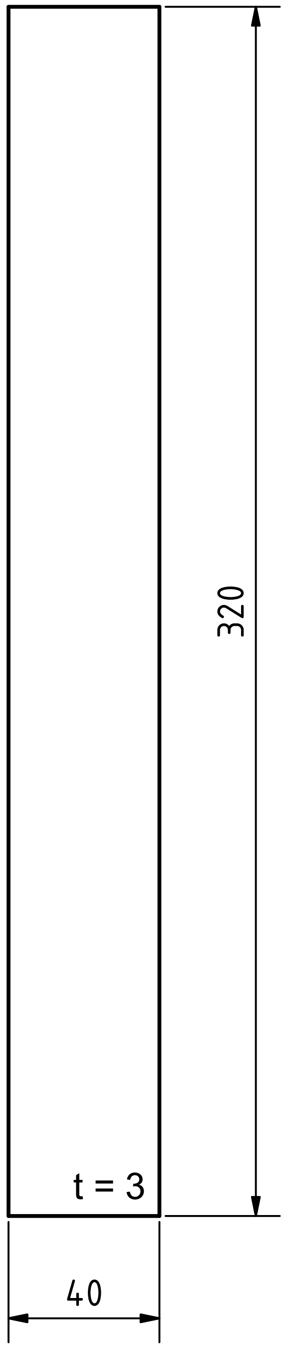

3 x for one drawer

Rz 63

General tolerance according to DIN ISO 2768 - mK		Scale 1:2	Material X8CrNiS18-9 (1.4305)
		Drying Chamber	

	Date	Name	
Author	20.04.2018	L. Büscher	Bulkhead
Checked			
Approved			

Status	Changes	Date	Name

HOCHSCHULE HANNOVER UNIVERSITY OF APPLIED SCIENCES AND ARTS

TAMK TAMPERE UNIVERSITY OF APPLIED SCIENCES

1

A4

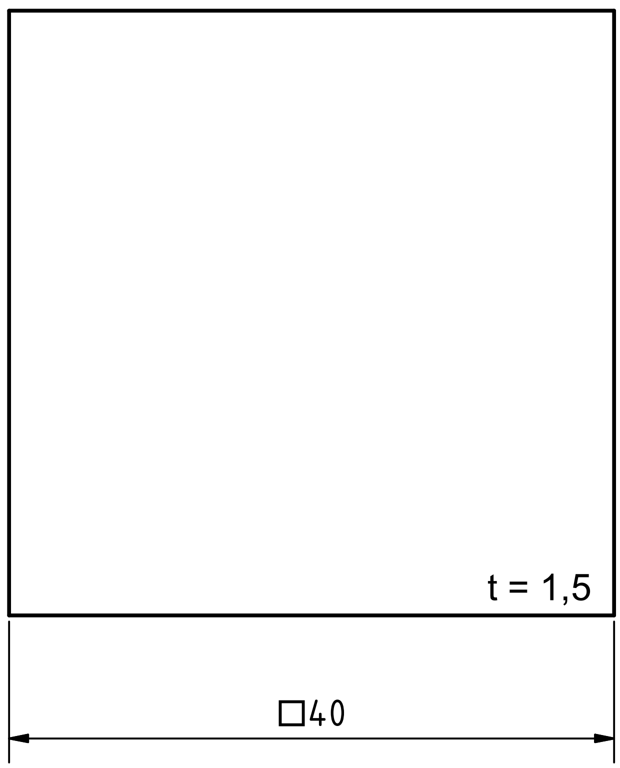

18 x

Rz 63 (✓)

General tolerance according to DIN ISO 2768 - mK		Scale 2:1	Material X8CrNiS18-9 (1.4305)
		Drying Chamber	

	Date	Name
Author	21.04.2018	L. Büscher
Checked		
Approved		

Stopper Drawer

HOCHSCHULE HANNOVER UNIVERSITY OF APPLIED SCIENCES AND ARTS

TAMPERE UNIVERSITY OF APPLIED SCIENCES

1

A4

Status	Changes	Date	Name

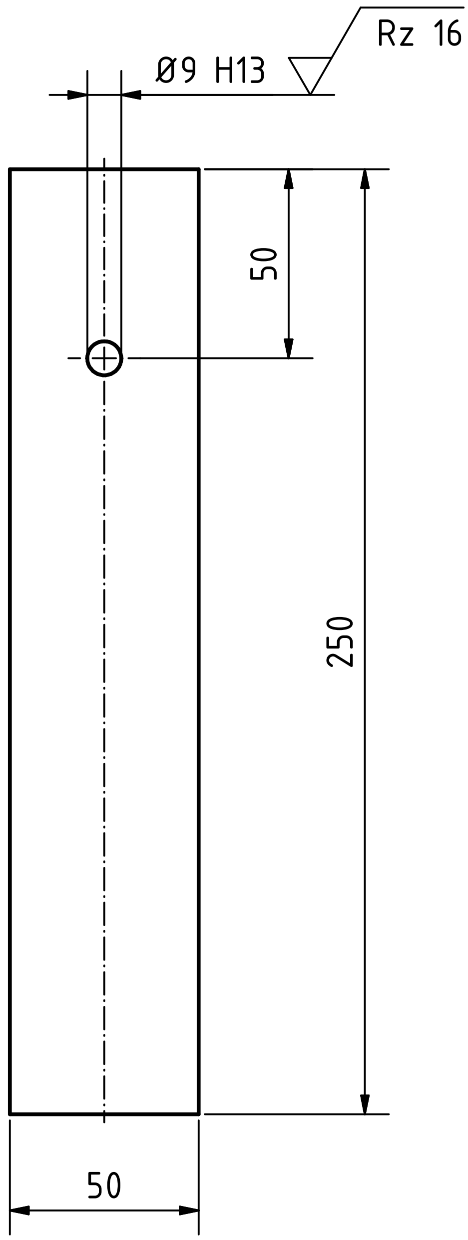

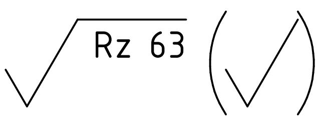

General tolerance according to DIN ISO 2768 - mK

Scale	1:2	Material	X8CrNiS18-9 (1.4305)

Drying Chamber

	Date	Name
Author	20.04.2018	L. Büscher
Checked		
Approved		

Arm

HOCHSCHULE HANNOVER UNIVERSITY OF APPLIED SCIENCES AND ARTS

TAMPERE UNIVERSITY OF APPLIED SCIENCES

1

A4

Status	Changes	Date	Name

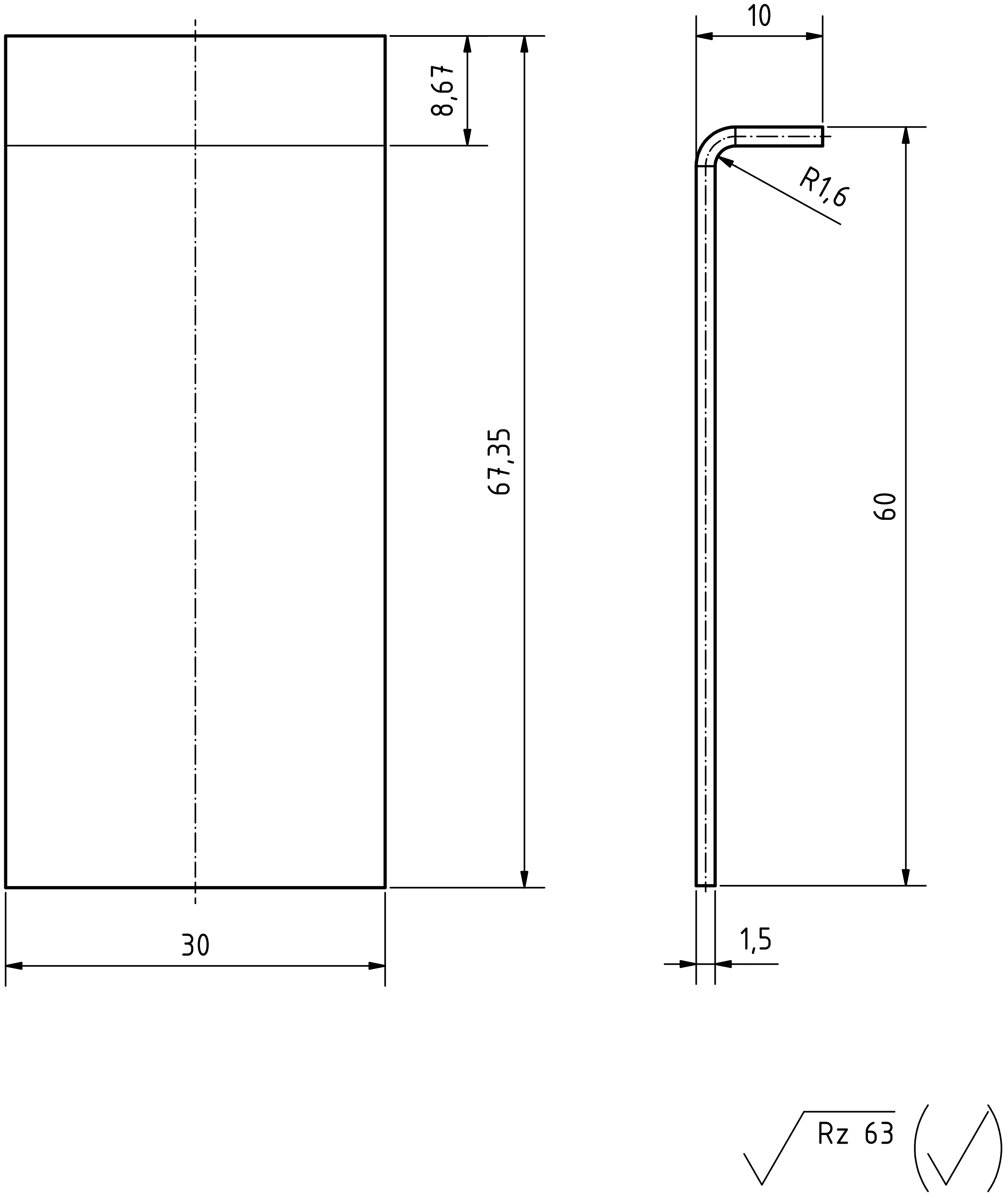

General tolerance according to DIN ISO 2768 - mK

Scale	2:1	Material X8CrNiS18-9 (1.4305)

Drying Chamber

	Date	Name
Author	21.04.2018	L. Büscher
Checked		
Approved		

Stopper Arm

HOCHSCHULE HANNOVER UNIVERSITY OF APPLIED SCIENCES AND ARTS

TAMPERE UNIVERSITY OF APPLIED SCIENCES

1

A4

Status	Changes	Date	Name

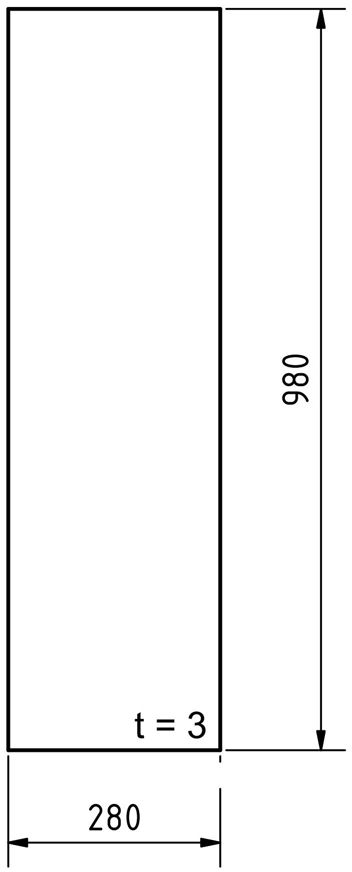

Rz 63 (✓)

General tolerance according to DIN ISO 2768 - mK

Scale	1:10	Material	X8CrNiS18-9 (1.4305)

Drying Chamber

	Date	Name
Author	20.04.2018	L. Büscher
Checked		
Approved		

Deflecting plate

HOCHSCHULE HANNOVER UNIVERSITY OF APPLIED SCIENCES AND ARTS

TAMPERE UNIVERSITY OF APPLIED SCIENCES

1

A4

Status	Changes	Date	Name

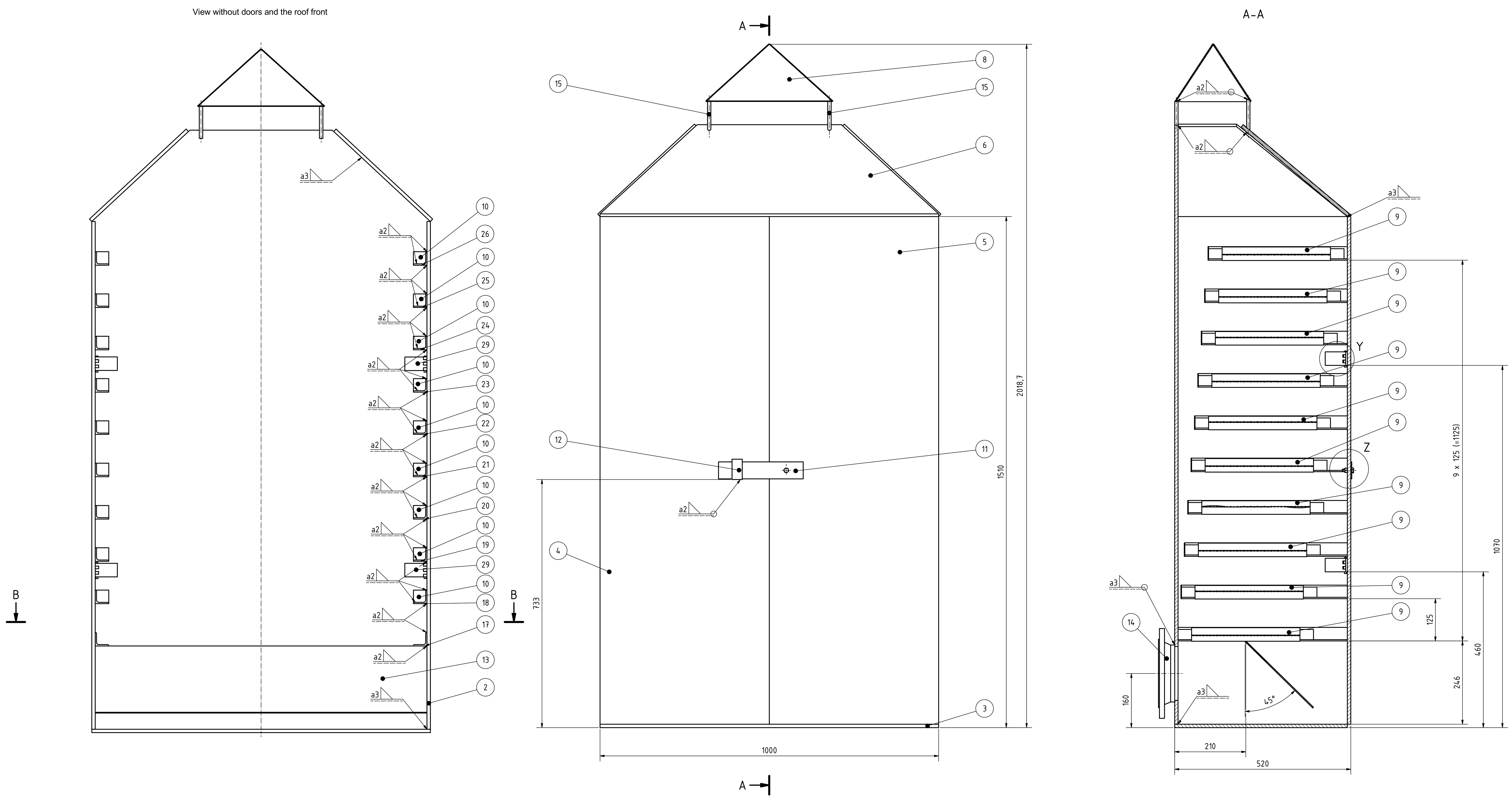

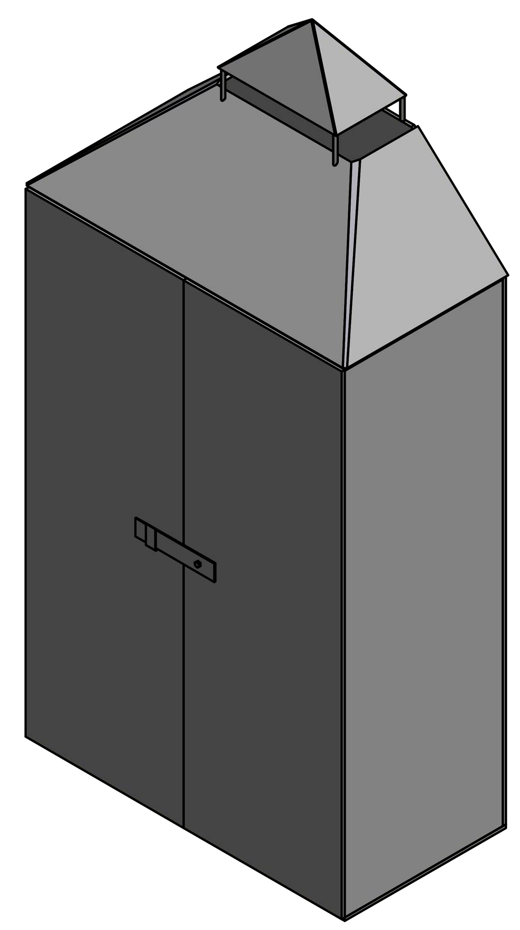

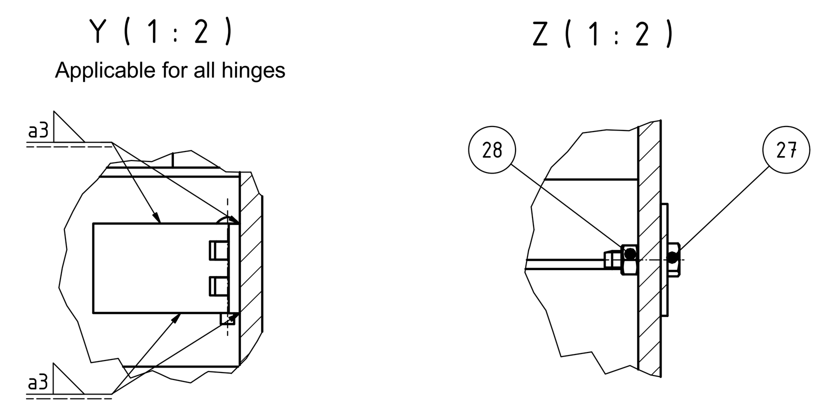

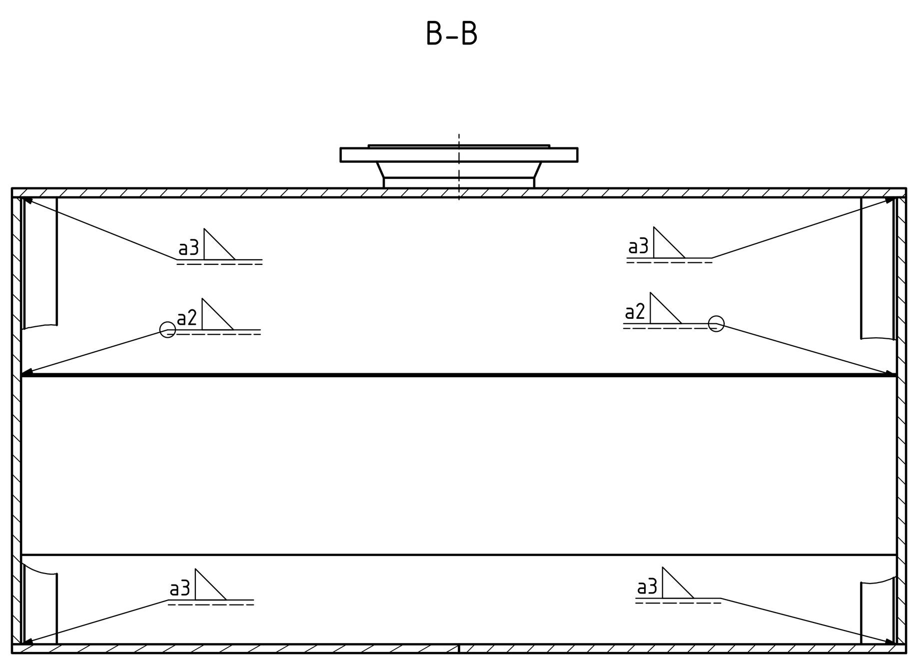

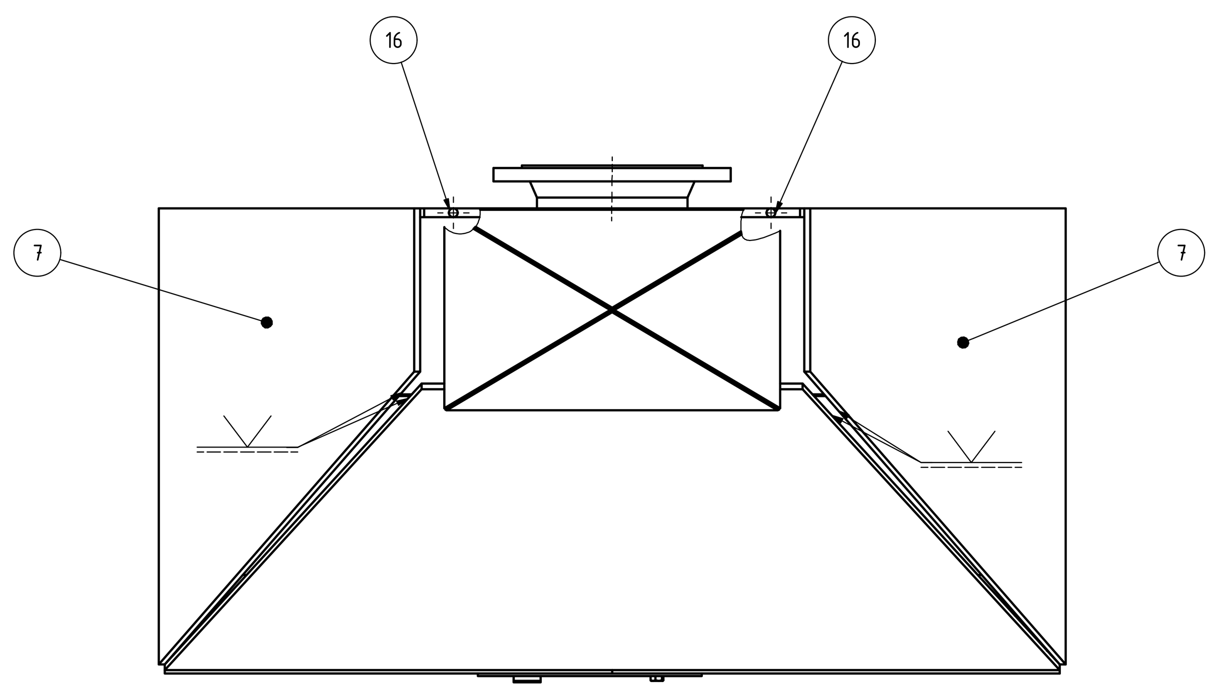

BAUTEILLISTE			
Pos.-Number	Quantity	Components Name	Details
1	1	Wall back	
2	2	Wall side	
3	1	Bottom Plate	
4	1	Door left	
5	1	Door right	
6	1	Roof front	
7	2	Roof side	
8	1	Caping	
9	10	Drawer	
10	18	Stopper Drawer	
11	1	Arm	
12	1	Stopper Arm	
13	1	Deflecting Plate	
14	1	Welding neck flange	DIN EN 1092-1 Typ 11 - PN 6 150 x 168.3
15	200 mm	Rod	DIN EN 10060 - 10 - 100
16	140 mm	Rod	DIN EN 10060 - 10 - 70
17	1000 mm	Equal angle squared edge steel	BS EN 10056-1 - L40x40x4-500
18	980 mm	Equal angle squared edge steel	BS EN 10056-1 - L40x40x4-490
19	960 mm	Equal angle squared edge steel	BS EN 10056-1 - L40x40x4-480
20	940 mm	Equal angle squared edge steel	BS EN 10056-1 - L40x40x4-470
21	920 mm	Equal angle squared edge steel	BS EN 10056-1 - L40x40x4-460
22	900 mm	Equal angle squared edge steel	BS EN 10056-1 - L40x40x4-450
23	880 mm	Equal angle squared edge steel	BS EN 10056-1 - L40x40x4-440
24	860 mm	Equal angle squared edge steel	BS EN 10056-1 - L40x40x4-430
25	840 mm	Equal angle squared edge steel	BS EN 10056-1 - L40x40x4-420
26	820 mm	Equal angle squared edge steel	BS EN 10056-1 - L40x40x4-410
27	1	Hexagon fit bolt with long spigot pipe thread	DIN 609 - M8 x 28-13
28	1	hexagon nut	DIN EN ISO 4033 - M8
29	4	weldable Hinge	60 x 40 x 5 - 60 x 40 x 5

General tolerance according to DIN ISO 2768 - mK

Scale 1:5 (1:2)

Drying Chamber

	Date	Name
Author	21.04.2018	L. Büscher
Checked		
Approved		

Drying Chamber

1

A0

Status | Changes | Date | Name